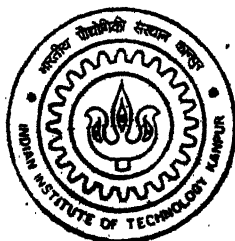


Optimization of a car suspension system using multi-objective genetic algorithms

by
Saket Awasthi



TH
ME/2001/m
A140

**DEPARTMENT OF MECHANICAL ENGINEERING
INDIAN INSTITUTE OF TECHNOLOGY, KANPUR**

January, 2001

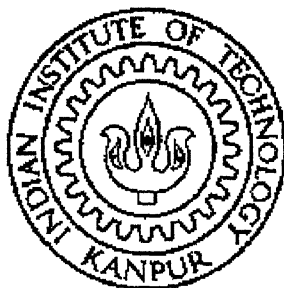
Optimization of a car suspension system using multi-objective genetic algorithms

A thesis submitted
in partial fulfillment of the requirements
for the degree of

Master of Technology

by

Saket Awasthi



to the

**Department of Mechanical Engineering
Indian Institute of Technology
Kanpur-208016, India
January, 2001**

16 APR 2001/ME

के द्वारा पुस्तकालय

का. प्रौ. वि. कातपुर

अवधि-क्र० A.133717

14/4/01
A.133717



A133717

Certificate

This is to certify that the work contained in the thesis entitled *Optimization of car suspension system using multi-objective genetic algorithms* by *Saket Awasthi* is carried out under supervision. This work has not been submitted elsewhere for a degree.



Kalyanmoy Deb
Professor
Deptt. of Mechanical Engg.
IIT Kanpur-208016



A. K. Mallik
Professor
Deptt. of Mechanical Engg.
IIT Kanpur-208016

Acknowledgment

I will like to express my sincere gratitude to my thesis supervisors Dr. A.K. Mallik and Dr. Kalyanmoy Deb. I am thankful to them for their continuous guidance and motivation during my thesis work. I have been fortunate to have them as my guides as they have been very patient and encouraging while clarifying my doubts. I could approach them any time of the day without hesitation and this has helped me immensely in completing my thesis work. There are many qualities that I would like to imbibe from them, hard work being one of them.

I will also like to thank my M.Tech batchmates Tushar Goel and Amit Gupta. Both of them have helped me a lot during my thesis work and I am extremely grateful to them. I wish to express my gratitude to other students in KanGAL, Sameer, Amrit and Mary who have helped me in improving my computer skills.

I also gratefully acknowledge the help of all of my friends at Hall—V who made my stay at IIT-Kanpur memorable. I also thank all the people who have directly or indirectly helped in the completion of the thesis.

Saket Awasthi

Abstract

Studying the dynamic response of a car suspension system and to find the optimal response to various kinds of excitations is one of the major challenges that the automobile industry is facing. The designer has to strike a balance between a vast number of objectives, many of them conflicting to each other, subject to several constraints and obtain an optimal solution which does not overlook any of the objectives.

The primary function of a suspension system in a car is to isolate the road excitations experienced by the wheels from being transferred to the passengers. In the present study we are considering an independent suspension system and we are assuming the part of the car above the chassis as a rigid body. The suspension system is modelled as two and three dimensional dynamic models. The car body is usually supported by a suspension spring and a damper at each wheel. The tyre of the wheel can be also assumed to have some stiffness in the vertical direction. The dynamic behaviour of a car suspension system is described by nonlinear differential equations of motion found from the free body diagram approach. The design variables are the stiffness and the damping parameters. Other parameters, which affect the dynamics of the car motion, like wheel to wheel distance, front and rear unsprung masses etc. are taken as constants. Different types of shocks, i.e., road excitations are applied to the wheel such as those caused by the wheels striking a bump, wheels striking a series of bumps, and that caused by the wheel's falling into a pot-hole etc.

A real world problem such as this poses many problems to the designer. Most of the conventional techniques are not suitable for this problem, as apriori knowledge of the car dynamics is required. Also, these processes are very time consuming and computationally expensive. Besides, there is a high probability that the results obtained are local in nature. The use of genetic algorithms overcomes the above mentioned difficulties and so the present study entails the use of genetic algorithms.

To start with a single objective such as maximum bouncing, pitching or rolling amplitude of the sprung mass is minimized subject to satisfying a number of constraints. The objective is expressed in terms of 'transmissibility' which is the ratio of maximum dynamic amplitude to the maximum excitation amplitude. Also, the objective function is considered in two different ways. Firstly, for optimization process we consider the time interval after the car has cleared the bump and in the second case we consider the whole period of travel including that on the bump. The constraints mainly arise from comfort considerations such as limiting the maximum vertical jerk experienced by the sprung mass, front and rear natural frequencies, and others. Even for a single constraint, restricting the maximum

vertical jerk, the feasible search space is found to be complex and multi-modal.

A real-coded genetic algorithm can successfully find near optimal solutions for different objectives. Since the search space is real the precision is more as compared to a binary coded genetic algorithm. The solutions obtained are better than a design that was being used in an automobile industry.

However, the solutions obtained by single objective optimization are not fully satisfying for practical applications. Dynamic system design can be formulated as a multi-objective problem. In the case of a car suspension design, the designer is faced with conflicting objectives such as minimization of maximum vertical displacement and minimization of maximum vertical acceleration. It has been observed that the smaller maximum vertical displacement leads to larger value of maximum vertical acceleration. So it is desirable to obtain a set of optimal solutions all equally good, from which the designer can choose a particular solution according to his requirement.

Non dominated sorting genetic algorithm-II (NSGA-II) can efficiently tackle the above multi-objective problem. This algorithm gives us a set of optimal solutions which takes care of both the conflicting objectives in a single run.

Under steady state excitations, the damper can be modelled as a linear system. However as the shock loading comes into picture the nonlinear property of the dampers come into play. So a non-linear cubic damping term was considered over and above the usual viscous damping term when the car was subjected to a rounded step displacement function.

Contents

1	Introduction	3
1.1	Introduction	3
1.2	A brief overview of previous work	5
1.3	Organisation of the present work	8
1.4	Closure	8
2	Vehicle Dynamics and Suspension Theory	9
2.1	Car suspension	9
2.1.1	Suspension modelling	10
2.1.2	Design concept	11
2.2	Suspension theory	11
2.2.1	Suspension elements	14
2.2.2	Suspension principles	15
2.3	Rigid body bounce/pitch motions	17
2.3.1	Interaction of front and rear suspensions to single applied disturbances	17
2.3.2	Effect of regularly repeated disturbances	18
2.3.3	Relative pitch and bounce frequencies k^2/l_1l_2 ratio	18
2.4	Non-linear suspension characteristics	19
2.5	Closure	20
3	Algorithms Used	21
3.1	Introduction to genetic algorithms	21
3.2	Standard genetic algorithm	21
3.2.1	Selection	22
3.2.2	Cross-over	22
3.2.3	Mutation	22
3.3	Real coded GA with SBX operator	24
3.4	Multi-objective genetic algorithm	26

3.5	Dominance	28
3.5.1	Dominance for unconstrained problems	28
3.5.2	Dominance for constrained problems	29
3.5.3	Constraint handling	29
3.6	Srinivas and Deb's non-dominated sorting genetic algorithm (NSGA)	30
3.7	Non-dominated sorting genetic algorithm-II (NSGA-II)	30
3.7.1	A fast non-dominated sorting approach	31
3.7.2	Density estimation	31
3.7.3	Crowded comparison operator	32
3.7.4	The main loop	32
3.8	Numerical integration algorithm	33
3.9	GA in conjunction with numerical integration algorithm	35
3.10	Closure	37
4	Car suspension models	38
4.1	Two dimensional model	38
4.1.1	Design variables and system constants	38
4.1.2	Mathematical modelling	40
4.1.3	Objective function	42
4.1.4	Constraints and variable bounds	43
4.1.5	Algorithm used	43
4.2	Three dimensional model	43
4.2.1	Design variables and system constants	44
4.2.2	Mathematical modelling	44
4.2.3	Objective function	48
4.2.4	Constraints	49
4.2.5	Non-linearity in damping parameters	50
4.2.6	Mathematical formulae used	50
4.2.7	Nondimensionalization of the differential equations	52
4.3	Closure	53
5	Results and Discussion	54
5.1	Two dimensional model	54
5.1.1	Single objective optimization results	54
5.1.2	Multi-objective optimization results	58

5.2	Results for three dimensional model	60
5.2.1	Single objective optimization	61
5.2.2	Results of multi-objective optimization	65
5.3	Conclusion	75
5.4	Scope for the future work	79
5.5	Closure	80
	Bibliography	81

List of Figures

2.1	Quarter car model	10
2.2	Simple coupled suspensions	12
2.3	Guest's model : Elastically conjugate points	12
2.4	Double conjugate points : A simple mathematical model	13
2.5	Mass diagram. $k^2/l_1l_2 = 1$	18
3.1	Simple genetic algorithm	23
3.2	SBX operator. probability distribution for the generation of children	25
3.3	The concept of Pareto-optimal solutions is illustrated.	28
3.4	The crowding distance calculation is as shown	32
3.5	Step doubling as a means for adaptive stepsize control in 4th order Runge-Kutta : points where the derivative is evaluated are shown as filled circles. The open circle represents the same derivatives as the filled circle immediately above it, so the total number of evaluations per step is 11 per two steps.	33
4.1	The dynamic model of the car suspension system, The above model has four degrees of freedom	39
4.2	Bilinear variation of rear suspension stiffness with deflection	40
4.3	A sinusoidal bump profile	42
4.4	A dynamic car suspension model with seven degrees of freedom	44
4.5	Single bump profile	47
4.6	Three bumps in series	47
4.7	Rounded displacement step function	48
5.1	Comparison of present and previous results for the case in which the bump time is excluded.	55
5.2	Comparison of real-coded GA and binary-coded GA results	56
5.3	Comparison of present and previous results for the case in which whole of time of travel is considered.	57

5.4	Comparison of two cases: one with bump time excluded and the other with bump time included.	58
5.5	The Pareto front showing the optimal values in objective space for the car speed of 5km/h . . .	59
5.6	Comparison of two extreme values on the Pareto-front for the car speed of 5 km/h . . .	60
5.7	The Pareto front showing the optimal values in objective space with a car speed of 25 km/h	61
5.8	Comparison of two extreme values on the Pareto-front for the car speed of 25 km/h . .	61
5.9	Results for single bump excitation at a speed 5 km/h	62
5.10	Results for single bump excitation at a speed 50 km/h	63
5.11	Results for three bumps excitation at a speed 5 km/h	63
5.12	Results for three bumps excitation at a speed 50 km/h	64
5.13	Results for rounded step excitation at a speed 5 km/h	65
5.14	Results for rounded step excitation at a speed 50 km/h	66
5.15	The Pareto front showing the optimal values in objective space for single bump at 50 km/h	67
5.16	The position of the Pareto-optimal front in the feasible search space in case of single bump excitation at speed 50 km/h	68
5.17	Results for single bump excitation at a speed 50 km/h	68
5.18	The Pareto front showing the optimal values in objective space for three bumps in series at 50 km/h	69
5.19	The position of the Pareto-optimal front in the feasible search space in case of three bumps excitation at car speed 50 km/h	70
5.20	Results for three bumps excitation at a speed 50 km/h	70
5.21	The Pareto front showing the optimal values in objective space for rounded displacement step at 5 km/h	71
5.22	Results for rounded displacement step excitation at a speed 5 km/h	72
5.23	The Pareto front showing the optimal values in objective space for rounded displacement step at 50 km/h	73
5.24	Results for rounded displacement step excitation at a speed 50 km/h	73
5.25	The Pareto front showing the optimal values in case of pitching motion for rounded displacement step at 50 km/h	74
5.26	Results for rounded displacement step excitation in case of pitching motion at a car speed 50 km/h	75
5.27	The Pareto front showing the optimal values in case of rolling motion for rounded displacement step at 50 km/h	76

5.28 Results for rounded displacement step excitation in case of rolling motion at a car speed	
50 km/h	76

List of Tables

5.1	Comparison of optimal values of stiffness and damping parameters for the case in which bump time is included.	55
5.2	Comparison of optimal values of stiffness and damping parameters obtained by using RGA and SGA	56
5.3	Comparison of optimal values of stiffness and damping parameters for the case in which whole of time of travel is considered.	57
5.4	Comparison of optimal values of stiffness and damping parameters for the two cases in which bump time is excluded or included.	58
5.5	Optimal values of stiffness and damping parameters with car speed 5 km/h	59
5.6	Optimal values of stiffness and damping parameters with car speed 25 km/h	60
5.7	Optimal values of stiffness and damping parameters for single bump excitation	62
5.8	Optimal values of stiffness and damping parameters for three bumps excitation	65
5.9	Optimal values of stiffness and damping parameters for rounded step excitation at speed 5 km/h	66
5.10	Optimal values of stiffness and damping parameters for rounded step excitation at speed 50 km/h	66
5.11	Optimal values of stiffness and damping parameters for single bump excitation at speed 50 km/h	69
5.12	Optimal values of stiffness and damping parameters for three bumps excitation at speed 50 km/h	71
5.13	Optimal values of stiffness and damping parameters for rounded displacement step excitation at speed 5 km/h	72
5.14	Optimal values of stiffness and damping parameters for rounded displacement step excitation at speed 50 km/h	74
5.15	Optimal values of stiffness and damping parameters for rounded displacement step excitation in case of pitching motion at speed 50 km/h	75

5.16 Optimal values of stiffness and damping parameters for rounded displacement step excitation in case of rolling motion at speed 50 km/h	77
---	----

Chapter 1

Introduction

1.1 Introduction

Design of dynamic systems is usually based on intuition and experience. Although industrial companies have started to switch from experimental studies to computational methods based on the multi-body system approach, design of mechanical systems is still largely carried out by intuitive changes of the design variables. This is due to the fact that the multi-body system approach is well developed for analyzing the dynamic behaviour of mechanical systems in a variety of disciplines, but there is a lack of tools for a systematic design via optimization. The optimization methods are not so popular with the design engineers in the industry mainly because most of them are not having wide range of use. They usually work very well for a certain kind of problems and fail miserably in the other cases. Secondly, most of them require a certain amount of apriori knowledge about the problem which is not always available to the designers. Thirdly, these methods require mathematical modelling of the real world problems which is not always easy. Also, these methods are very sensitive to the initial solution chosen and hence require a number of runs to obtain a global optimal solution. This makes these methods very time consuming and computationally expensive. However, genetic algorithms, which work on the nature's principle of the '*survival of the fittest*', can overcome all the above shortcomings of conventional optimization methods. In the present study the dynamics of a car suspension have been optimized using genetic algorithms.

Modelling and simulation in the field of vehicle dynamics is a complex topic. For the optimization of the vehicle's dynamic behaviour, not only model accuracy but also an efficient implementation of suitable approaches is of great importance. Practical work on this topic has resulted in integrated treatment of the mathematical modelling combined with adapted integration schemes. This approach also seems to be very well suited for applications in optimization.

Suspension systems are used to isolate the road excitations from being transmitted directly to the

passengers. Secondly they must do it without impairing the stability, steering or general handling qualities of the vehicle. A modern vehicle suspension system is a complex oscillatory system with a number of elasto-damping elements, the characteristics of which are in most cases of non-linear character. Due to the car's motion on the road and also to the effects of the power-train and the rotating elements, the vehicle performs stochastic, secondary, spatial oscillatory motion that affects the stability and comfort parameters, and may lead to fatigue of vital parts of the car, which in turn may threaten traffic safety. The negative effects of the secondary oscillatory motion can be reduced by way of optimization of characteristics of the elasto-damping elements of the vehicle.

Although different types of suspension systems exist, we consider here the design of an independent suspension system [1]. The suspension system parameters like stiffness of the springs and the damping coefficients of the dampers are treated as design variables. The optimization problem considers maximizing the ride comfort by minimizing the transmissibility and acceleration of the sprung mass when the suspension system is subjected to different kinds of base excitations.

In the present study, we consider both the two dimensional model and three dimensional model of the car. Firstly, we use real-coded genetic algorithm (RGA) [2], a single objective optimization algorithm, in conjunction with adaptive step-size control Runge-Kutta method [3], a numerical integration technique. The bounce motion of the car is considered and the minimization of transmissibility is considered to be the objective. A constraint limiting the value of maximum vertical jerk is used. The obtained results are compared with previously existing values of the design variables.

Since car-suspension design requires optimizing multiple objectives, many of which are conflicting to one another, it is desirable to have an optimization method which can effectively handle these objectives simultaneously. In the present study, we use the multi-objective genetic algorithm, Non dominated sorting genetic algorithm -II (NSGA-II) [4], for the purpose of optimization. It is used in conjunction with adaptive step size control Runge Kutta method, a numerical integration technique.

NSGA-II algorithm considers minimizing the vertical amplitude and minimizing the vertical acceleration as a set of conflicting objectives subjected to vertical jerk and frequency constraints. In case of three dimensional model, we also consider other set of objectives like pitching amplitude and pitching acceleration, rolling amplitude and rolling acceleration. The constraint limiting the maximum allowable vertical jerk experienced by the sprung mass is considered. The front, rear and pitching natural frequencies are limited to a lower and an upper bound. Finally in order to dampen the pitching motion

faster, the natural frequency of the front suspension system is kept smaller than that of the rear. Also, the variable bounds are fixed in order to avoid extra soft suspension. This leads to better handling and control of the car. Different kinds of road excitations like a sinusoidal bump, a series of bumps, and a rounded step displacement function etc. are considered. To take into account the transient response characteristics of a damper, cubic non-linear damping term is considered in addition to the usual viscous damping term [6]. The successful application of NSGA-II suggests that it is an efficient method for handling dynamic system design problems in mechanical engineering. The same software can be used for different design objectives for a car suspension by a small modification in the objectives and the constraints definitions.

1.2 A brief overview of previous work

C.N. Spentzas used Box's method [7] to determine the elastic and damping characteristics of a vehicle suspension that optimize the ride characteristics of a car. A seven degrees of freedom vehicle model was used and springs and dampers with non-linear characteristics were considered. Objective function considered vertical and rotational accelerations of the vehicle, permitting the optimization of ride characteristics. Also, by adding a term in the objective function related to the dynamic tyre load variation, the handling behaviour of the vehicle was simultaneously optimized. Only the rattle space constraint was considered. Only one objective was considered while optimization and other conflicting objectives were ignored. The jerk constraints (for comfort ride) and the frequency constraints were not considered. Also, the process is computationally expensive and time consuming. Using Box's method for optimization of non-linear springs and non-linear dampers, with so complex a model required a powerful computer and long computation time. Consequently, the use of seven degrees of freedom model was not justified from an engineering point of view. So, the use of four degrees of model was suggested, while still considering non-linear springs, non-linear dampers and large oscillations of the vehicle.

Miroslav Demic [8] optimized the characteristics of the elastic-damping elements of a passenger car by means of a modified Nelder-Mead method (Rao, 1984). In the work reported in the paper, the author modified the method of Nelder-Mead by introducing design-dependent bounds on the oscillatory parameter values. These values were computed on the condition that the object function has minimum, that the resonant frequencies of the aforementioned masses are located within the recommended bounds, and that the oscillatory parameters are within the prescribed bounds. The parameters computed provide for optimal comfort of the vehicle considered when driving on asphalt roads at high speeds of about 30 m/s. He applied this method to the plane model of a passenger car in order to minimize simultaneously vertical oscillations of the front and rear wheels, pitch, and vertical oscillations of a partially loaded

vehicle. No frequency or jerk constraints were chosen. Further, since simplex search method was used, the obtained solution was dependent on the initial solutions. There is a high probability that the algorithm may lead to a local optimum.

In another paper, Demic [7] directed his preference towards a modified version of the Hooke-Jeeves method, seeking the optimization of the characteristics of the elasto-damping elements of cars from the aspect not only of ride properties, but also of handling. Delimitation of the range of the optimization parameters was achieved by incorporating constraints to the algorithm by means of external penalty functions. The vehicle model that was used was obtained by extending the classic seven degrees of freedom model (bounce, roll, pitch motion of the sprung mass and bounce of the four unsprung masses) to a ten degree of freedom one. The three supplementary degrees of freedom (forward displacement, lateral displacement and yaw angle) permit the handling behaviour to be taken into consideration. But, since the matrix of transformation of co-ordinates from the body-fixed co-ordinates system to the ground-fixed co-ordinate system was linearized, only small displacements of the vehicle could be considered and the study of extreme situations either for the ride behaviour or for handling is not possible.

Another approach to this problem was presented by Pintado and Benitez [7] who used the linear programming method. The problem was solved in the time domain and also in the frequency domain, for deterministic and random excitations. But their approach considered only linear springs and dampers and this fact restricted the practical interest of the method, since most cars now-a-days use non-linear springs and dampers.

Wimmer and Rauth [9] formulated the car suspension system as a multi-criteria optimization of maximizing safety as well as maximizing the ride comfort. The optimal points were found by scalarization of the vector optimization problem. Frequently used scalarization approaches are the weighting criteria method, the global criterion method, the weighting min-max method, and the hierarchical optimization method, respectively. The remaining single criterion optimization problem was solved by standard optimization algorithms. However no aspects related to the jerk or frequency of oscillation of the passengers were considered.

Markine et al. [10] considered a finite element model of a truck and formulated an optimization problem with the location of various elements at the suspension system as design variables. The dynamic behaviour of truck was approximated by linear finite element models (both 2-D and 3-D). The road surface profile was presented as a random function with known power spectral density. The design

variables comprise geometry as well as spring and damper properties. Limitations were imposed on maximum values of the relative displacements of suspensions, dynamic wheel load to axles, acceleration of the car. A multi-point approximation method was used.

Also, Dieter Bestle and Peter Ebehard in their paper [11] considered optimization of a vehicle suspension system. They considered two conflicting objectives, pitching acceleration and vertical acceleration and used non linear programming along with a numerical integration technique to obtain optimal solutions. However, they used the weighted objectives method as a representative of the scalarization principle. Although here the hierarchical strategy converged to optimal points, the problem of local minima existed.

None of the above studies discussed the complexity of the feasible search space in a car suspension design problem. Due to nonlinear interactions of design variables and the requirement of solving a set of nonlinear differential equations governing the car, the search space in these problems is usually complex and multi-modal.

Deb and saxena used a simple binary coded genetic algorithm [1] as an optimization tool to find the optimal suspension system for a number of objectives such as minimizing bouncing, pitching and rolling amplitudes. Frequency and jerk constraints were also considered. The advantage of using genetic algorithms was manifold. It can be easily compounded with a numerical integration technique to obtain the optimal solutions. Secondly, unlike other conventional techniques this algorithm starts with a set of solutions and does not mislead us to a local optima. The solution obtained is a global solution and is independent of the initial set of solutions. Thirdly, no derivative information is required to reach to the optima. Also, it is computationally lesser expensive and lesser time consuming.

However solutions obtained with such an approach are not fully satisfying for practical applications, since they take into consideration only a single aspect out of a couple of conflicting system requirements or objectives. The present work deals with the car suspension optimization problem in a multi-objective context. The multi-objective approach seems to offer a promising way to change experimental system design to computer-aided design. Important, however, is that in context of multi-body system design dynamics criteria are highly nonlinear and their evaluation is rather time consuming since it involves numerical integration of differential equations of motion. It is in the above context that we see that multi-objective genetic algorithms are superior to conventional multi-objective optimization algorithms. Non dominated sorting genetic algorithm -II(NSGA-II) is capable of providing the global optima in a

single run.

1.3 Organisation of the present work

The present study is divided into five chapters. An outline of the five chapters is presented below :

- Chapter 1 : This gives a brief introduction of the present work and discusses the previous work and their shortcomings in brief.
- Chapter 2 : This chapter deals with the study of vehicle dynamics and suspension theory. Design concept and suspension principles are also discussed. A qualitative study of the suspension parameters and their characteristics is made.
- Chapter3 : This chapter presents a study of the various algorithms that are used in the present work. This also elaborates their usefulness for the present work and presents a step by step procedure for the way they are used in the present study.
- Chapter 4 : This chapter deals with the problem formulation and its statement. A detailed description of the two dimensional and three dimensional models used is given.
- Chapter 5 : This chapter presents the results of optimization of both two-dimensional model and three dimensional model and the inferences of the results are discussed qualitatively. Also, a scope for future work is presented and the conclusion of the whole study is given.

1.4 Closure

In this chapter we have given a brief introduction to the present work. A brief qualitative study of the previous work on the topic is also done. A comparative study of the previous work with the present work clearly indicates that shortcomings like the availability of a suitable multi-objective optimization algorithm, inadequate results owing to local optima, apriori knowledge of the real life problems, high computational time etc. are overcome in the present study. This also points to suitability of multi-objective genetic algorithms to the multi-body dynamics problems in the engineering field.

Chapter 2

Vehicle Dynamics and Suspension Theory

2.1 Car suspension

The primary function of the suspension system is to isolate the structure, so far as practicable, from shock loading and vibration due to irregularities of the road surface. Secondly, it must do this without impairing the stability of vehicle. The primary requirement is met by the use of flexible elements and dampers, while the second is achieved by controlling the relative motions between the unsprung masses, wheel and axle assemblies and the sprung masses. The diameter of the tyre, size of contact patch between tyre and road, the rate of the tyre acting as a spring, and weight of wheel and axle assembly affect the magnitude of the shock transmitted to the axle, while the amplitude of the wheel motion is influenced by all these factors plus the rate of the suspension springs, damping effect of the shock absorbers, and the weights of the sprung and the unsprung masses. The unsprung mass can be loosely defined as that between the road and the main suspension springs, while the sprung mass is that supported on these suspension springs, though both may also include the weights of parts of the springs and linkages.

A systematic treatment of the vehicle as a dynamic system best starts with the basic properties of a vehicle on its suspension system—i.e., the motions of the body and the axles. At low frequencies the body which is considered to be the sprung mass portion of the vehicle, moves as an integral unit on the suspensions. This is the rigid body motion. The axles and associated wheel hardware, which form the unsprung masses, also move as rigid bodies and consequently impose excitation forces on the sprung mass.

The dynamic behaviour of a vehicle can be characterized most meaningfully by considering the input-output relationships. There can be different kind of inputs. The output of interest is the vibrations of

the body. The ratio of output and input amplitudes represents a “*gain*” for the dynamic system. The term transmissibility is often used to denote the gain. Transmissibility is the nondimensionalised ratio of response amplitude to excitation amplitude in steady state forced vibration.

2.1.1 Suspension modelling

Different approaches for the modelling of suspension systems are used. As an example for different modelling approaches, the vehicle’s suspension characteristics are considered. Generally suspension models can be assigned to three different categories :

- kinematic models
- combined kinematic and elasto-kinematic models
- combined kinematic and elasto-kinematic models including inertia properties.

Road excitations are transmitted to the passengers through tyres, suspension system, chassis, car body, and the seat. Although this requires a detailed modelling of the interactions of each of these components, we limit our study only to the suspension system. Since an optimization procedure requires iterative evaluation of many solutions, this simplification reduces the computational complexity and helps to achieve the optimal solution quickly . If necessary, a local search with a detailed model may be performed in the vicinity of this solution to improve the solution accuracy. In this study we perform the former optimization only.

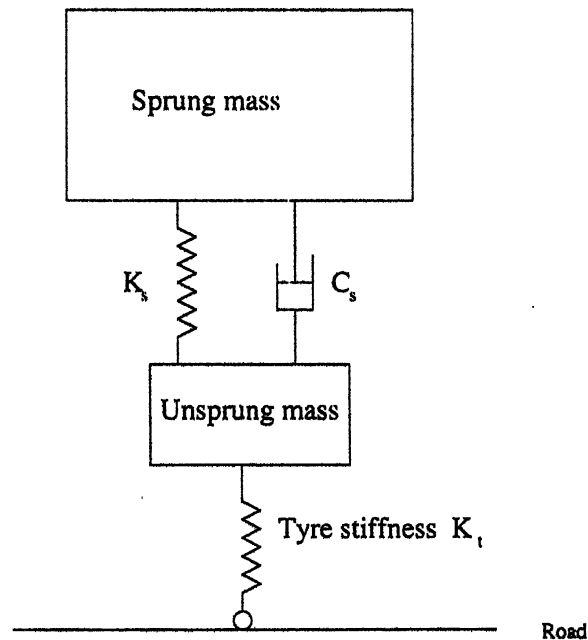


Figure 2.1: Quarter car model

A simplified vehicle suspension system or a quarter car model is shown in the figure 2.1. In the modelling of a suspension system, each tyre is modelled as a spring and is connected to the axle having an unsprung mass. The road excitation is transmitted to the axle through the tyre. Each axle is connected to the main body of the car, which is called the sprung mass, through suspension coils and dampers. Although the passenger seat is connected to the main car body through flexible connectors, we shall ignore them in this study and only concentrate on the effect of car suspension systems on the motion of the sprung mass.

2.1.2 Design concept

An integrated design approach for dynamical systems has to support all steps from problem formulation to problem solution by optimization. Firstly the technical system to be optimized are transformed to a mathematical model. The multi-body system approach is widely used in vehicle dynamics. Then, design goals are defined which is often difficult, since technical requirements and human wishes are sometimes difficult to be formulated as mathematical functions. Besides the complexity of the models this is maybe one of the reasons why even integrated design methods cannot substitute a design engineer, but support by software systems helps to make design better. In order to improve technical systems, design changes have to be made. Therefore, parameters of the model are classified either as design variables whose values can be varied for optimization process or as system constants whose values are fixed during optimization. In our study we consider the sprung mass, unsprung masses, wheel to wheel distances as the system constants and the stiffness and the damping parameters as the design variables. After all these preparations the optimization part of the design process may be started. In case of several objectives, a multi-objective approach is applied.

2.2 Suspension theory

When a rigid body, such as a car body, is mounted on springs at both ends, and the front springs are subjected to vertical forces through the front wheels, oscillations are produced in both front and rear springs. A similar action occurs when the vertical forces are applied to the rear wheels. One of the earliest treatments of this reaction between front and rear suspensions was presented by Professor J.J. Guest [12].

For simplification, lateral forces are not considered. Moreover it is also assumed that both front wheels are subjected to identical vertical forces simultaneously. The same conditions of identical forces also apply to the rear springs. The mathematical model is, therefore identical to two pogo sticks connected by a rigid bar as shown in the figure 2.2. Guest's model is shown in the figure 2.3. If a vertical force is applied at the front end of the beam, the line XY which represents the center line of the body,

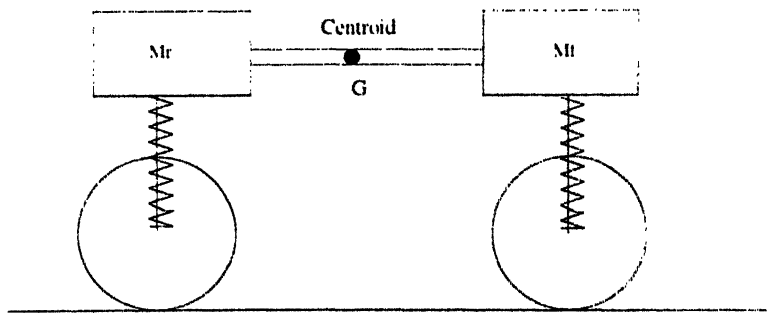


Figure 2.2: Simple coupled suspensions

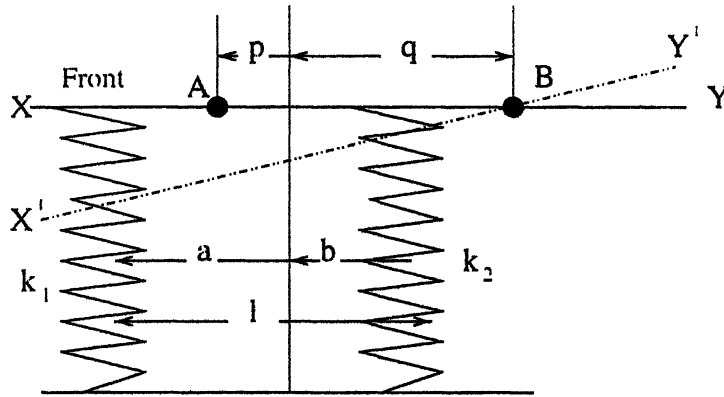


Figure 2.3: Guest's model : Elastically conjugate points

will adopt an inclined position $X'Y'$, rotating about point B . If a vertical force is applied at the rear, then rotation will be about point A . Any pair of points that possesses this relationship can be shown to satisfy the equation $pq = ab$. The dimensions a and b are established by the relative rates of the front and rear springs k_1 and k_2 , since $k_1 a = k_2 b$. The spring center C is, therefore, the point of balance and a vertical force applied at C will lift the beam with no tendency to tilt. Points A and B are called *elastically conjugate points*.

The next stage of the Guest construction [12] is the *dynamically conjugate points* of the sprung mass. The moment of inertia of the sprung mass about the centroid is MK^2 . The sprung mass M for which $I_g = MK^2$ can be represented by discrete masses m_1 and m_2 at distances r and s from the centroid G . To satisfy the equation, $rs = K^2$, the following conditions must be met:

$$\begin{aligned} m_1 + m_2 &= M, \\ m_1 r &= m_2 s, \\ m_1 r^2 + m_2 s^2 &= MK^2. \end{aligned}$$

As in the case of the elastically conjugate points, the quantity r is chosen arbitrarily and the corresponding value of s is found from the relationship $rs = K^2$. Just like the elastically conjugate

points there are infinite number of dynamically conjugate points.

The final stage is to combine the two systems. This will give us the *double conjugate points* that will satisfy both conditions. There is only one such pair of points.

To calculate double conjugate points, the following information is used.

$$pq = c^2 = ab.$$

$$rs = K^2.$$

$$p = r + x.$$

$$q = s - x.$$

$$a = \frac{k_2}{(k_1 + k_2)} L.$$

$$b = \frac{k_1}{(k_1 + k_2)} L.$$

where x is the distance between the center of gravity ' G ' and the spring center ' C ', a and b are the distances of the spring center from the front and rear wheels. L is the distance between the front and the rear axles and k_1 and k_2 are the front and rear spring rates respectively. In figure 2.4, G is the

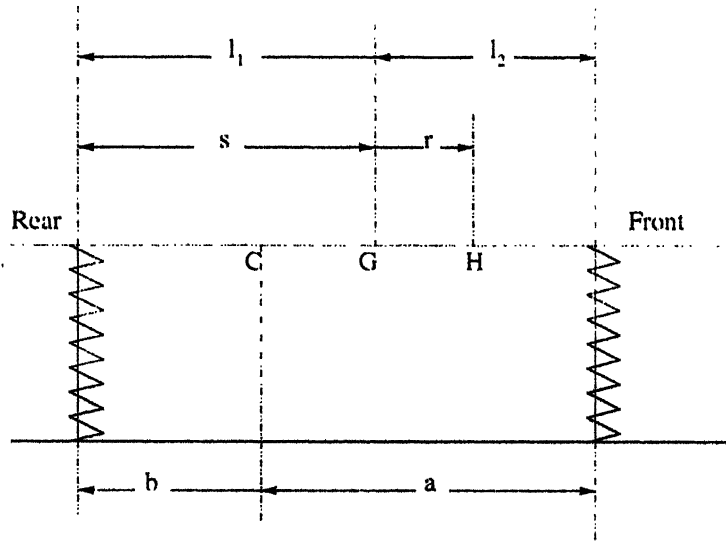


Figure 2.4: Double conjugate points : A simple mathematical model

centre of gravity, C is the spring centre, and H is the conjugate centre.

K^2 is a quantity that is measured experimentally. Usually it is taken as

$$K^2 = l_1 l_2,$$

where l_1 and l_2 are the distances of the center of gravity from the front and rear axles.

From the above equations we get,

$$r = \frac{K^2 - x^2 - ab}{2x} + \frac{\sqrt{(K^2 - x^2 - ab)^2 + 4K^2 x^2}}{2x}$$

A few special cases are discussed below :

- Most modern vehicles with substantial front and rear overhang exhibit dynamic index close to unity. That is :

$$DI = K^2/l_1l_2 = 1$$

When the equality holds, the front and rear suspensions are located at conjugate centers of percussion (an input at one suspension causes no reaction at the other). In this case the oscillation centers are located at the front and rear axles. This is a desirable condition for good ride as there is no interaction between the front and the rear suspensions. Some special cases are discussed now [13]:

- Spring center at the CG---This condition corresponds to the case of coupled pitch and bounce motions. The pitch and bounce oscillations are totally independent. Poor ride results because the motions can be very irregular.
- Dynamic index K greater than unity - This occurs when there is substantial overhang at the front and/or rear end of the car. The bounce center is in front of the CG (beyond the front axle) and the pitch center is between the CG and the rear axle. The natural frequency and flat ride will still result if the spring center is located far enough behind the CG (front ride rate less than rear ride rate).
- Uncoupled motion and dynamic index equal to one - This condition results in equal bounce and pitch frequencies. The ride is inferior because there is essentially no pattern to the road-generated motion; it is quite unpredictable.

2.2.1 Suspension elements

The suspension elements present in the model are the springs and the dampers. The suspension spring is in series with a relatively stiff tyre spring, so the suspension spring predominates in establishing the ride rate and, hence, the natural frequency of the system in the bounce (vertical) mode. Therefore, in the present study we have considered tyre stiffness as a system constant while the suspension spring stiffness is a design variable. Since road acceleration inputs increase in amplitude at higher frequencies, the best suspension is achieved by keeping the natural frequency as low as possible. For a vehicle with a given weight, it is therefore desirable to use the lowest possible spring rate to minimize the natural frequency. A softer spring leads to lower acceleration but the spring stiffnesses are usually kept above certain values to make the ride handling easier.

Dampers are used to make the vibrations die down. In absence of damping a vibration once excited would exist indefinitely. In practice damping exists in three forms : friction, viscous and that due to the presence of air. The suspension of most vehicles exists to keep to a minimum the disturbances of the sprung body due to irregularities in the terrain over which the vehicle runs. Friction, in the suspension linkage, means that no movement of the suspension itself occurs for irregularities below those at which the deflection of the tyre implies an increase in force equal to static friction force. This constitutes only a small component of the total damping. Damping due to air is also small compared with that necessary to prevent unduly large movements of the sprung weight and can equally be regarded as insignificant. The main bulk of damping is therefore likely to be viscous damping from the hydraulic dampers which are now universally used. It is referred to as viscous damping and taken as being proportional to the vertical velocity between unsprung and sprung masses because this is mathematically true and is reasonably close to the true state of affairs.

The amount of damping required is, as in so many cases in engineering, a compromise : in this case between that needed to prevent undue persistence of a vibration at natural frequency excited by a single disturbance, which also prevents the build-up of excessive amplitude of a forced vibration due to a series of impulses, and the uncomfortable fact that the higher the damping force the greater the disturbance fed into the sprung mass by any given road irregularity. The damping force is responsible for an additional disturbance on the sprung weight over and above that due to the deflection of the suspension spring.

Of the two different frequencies : one is that of the sprung mass on the suspension spring system, and the second is that of the unsprung mass- the wheel and axle assembly- on the tyre. Obviously the latter is affected by the suspension spring rate, but only marginally. The former will be experienced as a relatively low frequency- perhaps about 1 to 2.5 Hz-bouncing of the carriage unit, while the latter is that of wheel hop, at a higher frequency-generally 10 to 15 Hz-and is generated almost totally independent of the motions of the carriage unit. For minimizing the amplitudes of wheel hop-not only resonant but also isolated hops- the unsprung weight must be kept as small as possible. Resonances of either the sprung or unsprung masses can affect adversely, and indeed to a dangerous extent, the handling characteristics of the vehicle. Obviously, therefore, it is important to maintain the dampers, or shock absorbers, in good working condition.

2.2.2 Suspension principles

Pure bounce will occur if the front and rear sprung masses are equal [14], the front and rear springs have identical frequencies and identical rates and are in phase. A car can be designed to have a 50/50

weight distribution and identical springs all around, but the phasing of ripples in the road surface are beyond our control. It is inevitable that a degree of pitching must often occur. The inertia of the sprung mass will resist this pitching motion and the disposition of the major components, i.e. the engine, transmission, fuel tank, passengers, etc., that make up the sprung mass contribute to the resistance exerted by the sprung in opposition to the pitching moment. If the major masses of the body components tend to be near the centroid, the sprung mass offers less resistance to pitching than a body of the same total mass that has the more massive components situated at a greater distance from the centroid. Expressed technically, we say that the second case has a larger polar moment of inertia. In the present study we are interested in two polar moments of inertia, i.e., pitching moment of inertia and rolling moment of inertia. Although many modern cars have the centroid well forward, the value of (K^2/l_1l_2) is often close to unity. This is more by chance than by deliberate design. K is the radius of gyration and l_1 and l_2 are the distances of the center of gravity from the front and rear axles respectively.

A general rule that is observed in a vehicle suspension design is that the rear natural frequency should be greater than the front natural frequency by at least 10 percent. This is rationalized by the observation that vehicle bounce is less annoying as a ride motion than pitch. Since excitation inputs from the road to a car affect the front wheels first, the higher rear to front ratio of frequencies will tend to induce bounce. Also the locations of the motion centers are dependent on the relative values of the natural frequencies of the front and rear suspensions. With equal frequencies it is found that one center is at the C.G. location and the other is at infinity. Equal frequencies correspond to decoupled vertical and pitch modes, and "pure" bounce and pitch motions result. With a higher front frequency the motion is coupled with the bounce center ahead of the front axle and the pitch center toward the rear axle. A lower front frequency puts the bounce center behind the rear axle and the pitch center forward near the front axle. This latter case was recognized by Maurice Olley in the 1930's [12] as the best for achieving good ride.

Since the suspension spring in series with a relatively stiff tyre spring, suspension spring predominates in establishing the ride rate and, hence, the natural frequency in the bounce (vertical) mode. Since road acceleration inputs increase in amplitude at higher frequencies, the best solution is achieved by keeping the natural frequency as low as possible. For vehicle with a given weight, it is therefore desirable to use the lowest practical suspension spring rate to minimize the natural frequency. However, the practical limits of stroke that can be accommodated within a given vehicle size and suspension envelope constrain the natural frequency for most cars to a minimum in the 1 to 1.5 Hz range. Performance cars on which ride is sacrificed for the handling benefits of a stiff suspension will have natural frequencies upto 2 or

2.5 Hz. In the present study, all the frequencies i.e. front, rear, pitching are constrained to a range of 0.8 to 2.5 Hz. This allows for a better handling of a car besides maintaining a good ride comfort level.

2.3 Rigid body bounce/pitch motions

The simple mechanics of the quarter-car model do not fully represent the rigid-body motions that may occur on a motor vehicle. Because of the longitudinal distance between the axles, it is a multi-input system that responds to the pitch motions as well as vertical bounce. This is the reason for considering the two dimensional model instead of a quarter-car model in the present study. Depending on the road and speed conditions, one or the other of the motions may be largely absent, or they may not necessarily be observed at the point on the vehicle where the vibration measurements are made. The pitch motions are important because they are generally considered objectionable and are the primary source of longitudinal vibrations at locations above the center of gravity. Understanding the pitch and bounce motions is essential because it is their combination that determines the vertical and longitudinal vibrations at any point on the vehicle.

2.3.1 Interaction of front and rear suspensions to single applied disturbances

A car may meet a single bump or hollow affecting one track only, or it may meet a transverse ridge or hollow affecting both tracks. If we consider a transverse ridge, as a result of passing over it the front end of the car is raised. Then, after an interval depending on the wheelbase and the speed, the back end of the car is raised.

The first effect of lifting of the car is to excite some pitch movement. The subsequent lifting of the back end of the car may mitigate or aggravate that pitch movement, depending on the time interval and the pitch frequency because the movement of the sprung weight on its suspension is not critically damped. any movement of the suspension at each end of the car will persist with diminishing amplitude for a number of oscillations. Depending on the relative frequencies of the front and rear suspensions and the amount of damping, the initial pitching motion may be reduced or increased by the passage of time. A few facts about the above case are listed below :

- With the lower frequency rear suspension there is a strongly persisting pitch movement.
- With the higher frequency rear suspension the initial pitch movement is very quickly reduced.
- With the higher frequency rear suspension the initial pitch movement is never so severe as with the lower frequency.

- The initial pitch movement is less severe at the higher than at the lower speed, because the time interval is less. This time interval is at both speeds less than half a cycle of the front suspension.

2.3.2 Effect of regularly repeated disturbances

Many road surfaces have developed fairly regularly occurring bumps and hollows. For a car traversing such a road the wheelbase filter effect has to be considered. In its simplest form, for condition where the vehicle wheelbase equals half the road disturbance wavelength, pitching is excited if the combination of vehicle speed and disturbance wavelength produces a disturbance frequency equal or close to the vehicle's pitch frequency. The extent to which the pitching amplitude builds up depends on the suspension damping factor. Some build up will also occur if the wheelbase is $3/2$, $5/2$ etc. times the disturbance wavelength and the vehicle speed produces impulses at or close to the vehicle pitch frequency. This effect considerably affects the vehicle's vertical acceleration spectra at the center of gravity and rear wheel positions, and the pitch acceleration spectra.

2.3.3 Relative pitch and bounce frequencies k^2/l_1l_2 ratio

Assuming that the frequency of oscillation is unaffected by pitching as opposed to bouncing movement of the car, this is generally nearly true. To be true the front and rear end masses would have to be effectively concentrated in front and rear axle vertical planes across the car. If this condition is met then the moment of inertia I of the car about a transverse axis through the centre of gravity as shown in the figure 2.5, is :

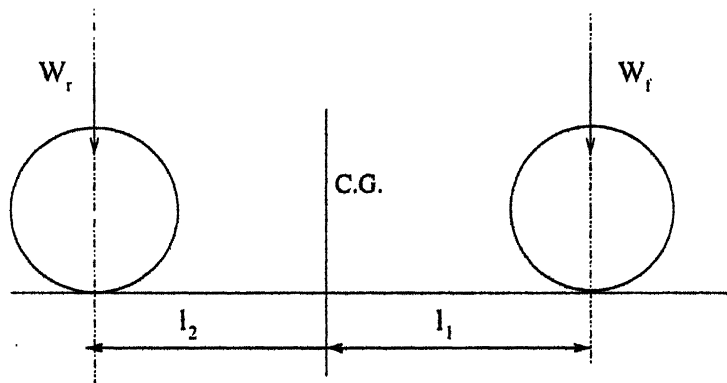


Figure 2.5: Mass diagram, $k^2/l_1l_2 = 1$

$$I = W_f l_1^2 + W_r l_2^2$$

Because a and b are the distances of the centre of gravity from the front and rear wheels

$$W_f l_1 = W_r l_2$$

Substituting in the second term of the moment of inertia equation, we get :

$$I = W_f l_1 (l_1 + l_2)$$

Now, $W_f = W l_2 / L$, so

$$I = W l_1 l_2 (l_1 + l_2) / L = W l_1 l_2$$

The usual expression for the inertia I of a body is $W K^2$ where K is the radius of gyration. It follows therefore that the ratio $K^2 / l_1 l_2$ as an indication of how far the car departs from the characteristic of equal pitch and bounce frequencies.

The fact that $K^2 / l_1 l_2$ is generally less than 1 has two effects :

- The pitch frequency is higher and therefore for given amplitudes the accelerations will be greater.
- Because the resistance to pitching is less a given exciting force will produce a greater amplitude of pitch. Looking at a vehicle suspension with tyre acting as a spring, the less the resistance of the sprung mass to the pitching motion resulting from a given road ridge as disturbance the less the tyre deflection and therefore greater the deflection of the vehicle suspension system and therefore the greater the initial pitch amplitude of the sprung mass on its suspension.

In ideal case $K^2 / l_1 l_2 = 1$ is used in the present study and the centroid is nearer to the front axle, so this combination leads to the faster dying down of pitching motion as it is the most irritating motion.

2.4 Non-linear suspension characteristics

Non-linearity is ubiquitous in nature [15]. Linearity is an approximation to reality. In shock and vibration systems, isolators such as air springs, elastomeric dampers, and wire-rope isolators are inherently nonlinear. Assumption of Hooke's law for springs and linear viscous damping for dampers is done just for mathematical simplicity. Sometimes the amplitudes of steady state vibration are small enough to justify the assumption of linearity. However, the transient displacements may often be sufficiently large when the non linearity in springs and dampers cannot be ignored.

It has been established that the effect of nonlinear damping is more predominant than the effect of nonlinear stiffness so far as the performance of shock isolators for base excitation is concerned [6]. In the present study a cubic non-linear damper is considered in addition to the linear viscous damper, in the case of shock excitation of the suspension system by a rounded step function. However, the stiffness characteristics are considered to be linear throughout. The damping force expression with non-linear

damping term is given as :

$$F = c_f \dot{d} + c_{fn} \dot{d}^3$$

2.5 Closure

In the present chapter we discussed the car suspension modelling and its design . To understand the present work properly a brief discussion on the suspension theory is made. The suspension principles are also mentioned as their knowledge is a must for the problem formulation. The suspension parameters are also studied in brief and their effect on the ride characteristics is also mentioned. A qualitative study of relationship between pitch and the bounce motions is made and the effect of dynamic index on these motions is also discussed. At the end of the chapter, non-linearity in the dampers is discussed briefly.

Chapter 3

Algorithms Used

3.1 Introduction to genetic algorithms

Genetic Algorithms (GA) are finding extensive use now-a-days in the field of optimization related problems. They form a very robust tool for the optimization part of computer aided design process. Genetic algorithms are more suited for optimization when used alongwith a numerical integration technique. In the present study we have used different kinds of genetic algorithms, i.e. real coded genetic algorithm and the multi-objective genetic algorithm. The genetic algorithms offer many advantages over the conventional methods of optimization. A few of the advantages are :

- Unlike conventional technique genetic algorithms are robust, i.e. they can be used efficiently for a wide range of problems.
- GAs are not sensitive to initial solution chosen.
- GAs do not require derivative or any such information.
- GAs are capable of finding global optimum in just one run.

3.2 Standard genetic algorithm

Genetic Algorithm(*GA*) is the optimization technique, which mimics the nature in order to find the global optima of a given problem. This is inspired from the concept of “*Survival of Fittest*”. It means that only those individuals, which are better than others in one or other aspect survive. Unlike classical optimization methods GA deal with a population of individuals. In Binary GA individuals are represented by the binary strings called chromosomes. These chromosomes are the string of 0's and 1's called *allele*. In Real Coded GA, chromosomes comprise of string of real numbers. Salient features of a standard simple GA are as following.

1. Selection.

2. Cross-over.

3. Mutation.

3.2.1 Selection

For a given population of individuals only those individuals are selected which are better in fitness than others. This way, GA follows the Darwinian law of survival of the fittest and by this selection our search is guided towards the optima. More importantly, this method does not reject the solution which is not the best. This solution may have the information, useful in finding the global best solution. Most used methods for selection are

1. Tournament Selection.

2. Stochastic Universal Sampling.

3. Roulette Wheel Selection.

3.2.2 Cross-over

In cross-over two individuals mate and produce children. This is a very important operator which create the new solutions, by using the properties of the parents. This create the solutions in the region other than the existing region. This explores the search space to find the best region. It is supposed that the individuals which are surviving, have some good string, which let them alive. So good parents combine to produce better children. Two types of crossovers are mostly used:

1. Binary Crossover.

Deals with chromosomes with binary numbers.

2. Real Crossover.

Deals with chromosomes with real numbers.

3.2.3 Mutation

This mimics the sudden changes occurring in the nature, that creates the individuals, different from the individuals of its own category. This operator is particularly helpful when the search has stuck at some local optima or search is going slowly. This can also create solutions which are not good. They will be taken care by the selection and other operators.

The algorithm of simple GA is shown in figure 3.1.

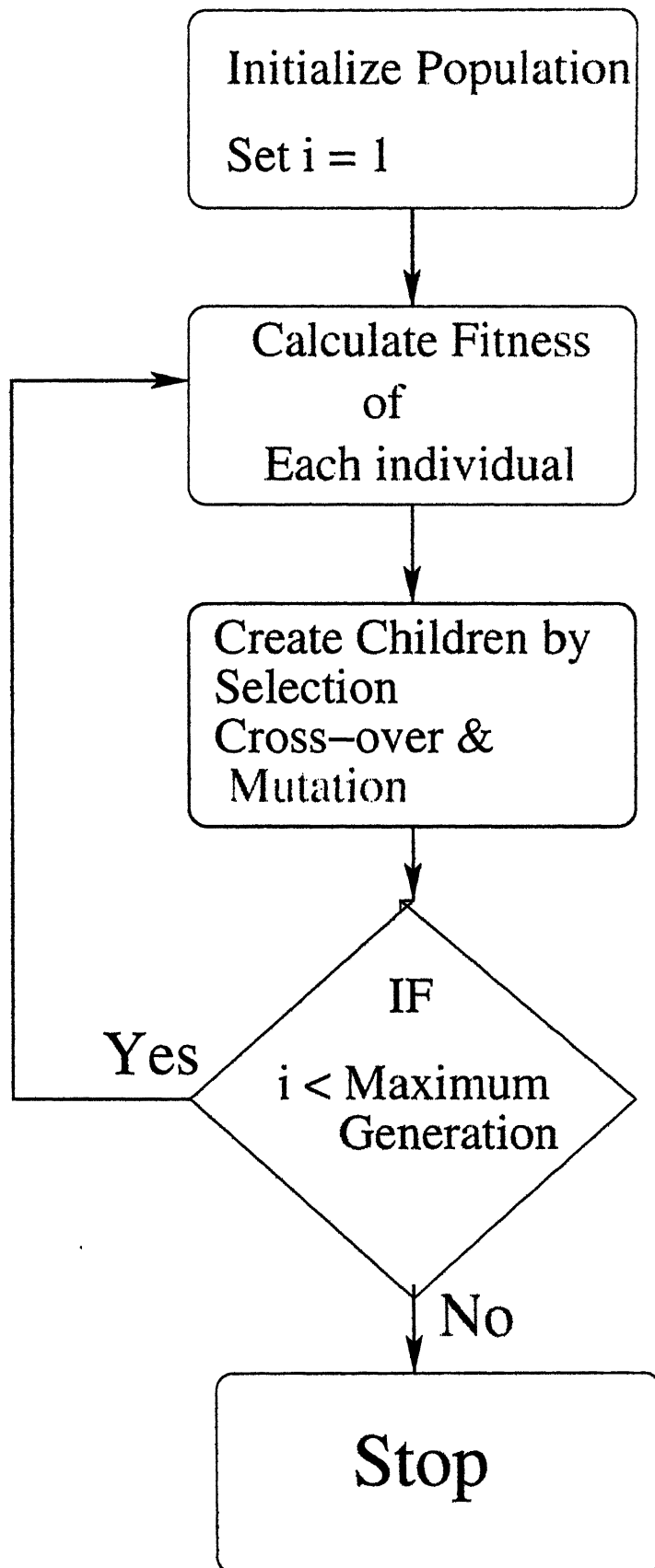


Figure 3.1: Simple genetic algorithm

3.3 Real coded GA with SBX operator

Binary coded GAs discretize the search space by using the coding of real variables in binary strings. However, the search space is real and continuous. The coding of real variables in finite-length strings causes a number of problems like:

- Inability to achieve arbitrary precision in obtained solution.
- Fixed mapping of problem variables.
- Inherent Hamming Cliff problem associated with binary coding.
- Processing of Holland's schemata in continuous search space.

To overcome all such difficulties the real coded GA (RGA) are used. In the present work, for single objective optimization an RGA using Simulated Binary Cross-over or SBX [2] has been used. This RGA employs a real-coded cross-over whose search power is similar to that of the single point cross-over used in binary-coded GAs. In order to achieve that we define the search power of a cross-over operator in terms of the probability distribution of any arbitrary child string to be created from any two given parent strings. The search power of the single-point cross-over operator is first calculated. Later, the simulated binary cross-over (SBX) is developed having a search power similar to that of the single-point cross-over. The difference in the implementations of the real coded GAs with SBX and binary-coded GAs with single-point cross-over is that in the former method the coding of variables is eliminated and a child string is created from a probability distribution that depends on the location of the parent strings.

In the case of simulated binary cross-over (SBX) a parameter called "*spread factor*", denoted by β is defined. Based on this parameter the cross-over operator can be of three types. Operators having $\beta < 1$ are called *contracting operators* and those having $\beta > 1$ are called *expanding operators*. The operators having $\beta = 1$ are termed as *stationary operators*. The random variate β is generated using the polynomial distribution as below,

$$p(\beta) = 0.5(\eta + 1)\beta^\eta, \quad \text{for } \beta \leq 1$$
$$p(\beta) = 0.5(\eta + 1)\frac{1}{\eta + 2}, \quad \text{for } \beta > 1$$

The value of "spread factor" is calculated by equating the area given by a randomly generated random number between 0 and 1 to above equations. The probability distribution curve is shown in figure 3.2. Here η is the distribution index of the probability distribution. After calculating β from above equations

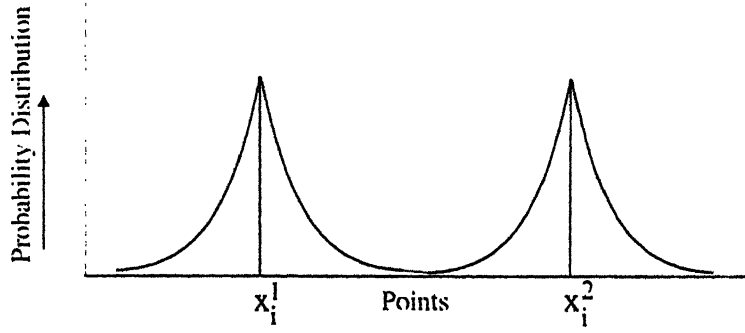


Figure 3.2: SBX operator. probability distribution for the generation of children

the children points are generated as follows :

$$y_i^1 = 0.5[(1 + \beta_i)x_i^1 + (1 - \beta_i)x_i^2]$$

$$y_i^2 = 0.5[(1 - \beta_i)x_i^1 + (1 + \beta_i)x_i^2]$$

Here β_i is defined as $\beta_i = |\frac{y_i^2 - y_i^1}{x_i^2 - x_i^1}|$. The spread factor is randomly generated from a polynomial distribution defined above for each variable in case of “variable by variable” crossover.

The β is generated by transformation of above polynomial distribution using uniform variate as follows.

$$\beta(u) = (2u)^{\frac{1}{\eta+1}}, \quad \text{if } u(0, 1) \leq 0.5$$

$$\beta(u) = [2(1 - u)]^{\frac{1}{\eta+1}}, \quad \text{if } u(0, 1) > 0.5$$

u is a uniformly generated random number between 0 and 1.

In case of multi-variable problems, the crossover is done “variable by variable” i.e. for a variable the crossover will take place with a probability 0.5. If the crossover is to be done the value of β is calculated using above equations.

The characteristic of the SBX operator is that it generates offsprings depending on the position of the parents. If the parents are far, the children solutions are created far away and if the parents are close the children are generated close. Also a small value of the distribution index creates points far away while a larger value gives closer solutions.

Simulated binary crossover for problems having no bounds on the variables has been described above. If the problem parameters have bounds, SBX can be used after some modification. In this case the area

of the probability distribution which lies outside the bounds is added to that is enclosed by the bounds. Mathematically it is done as follows.

$$\beta_q = (u\alpha)^{\frac{1}{q+1}}, \quad \text{if } u \leq \frac{1}{\alpha}$$

$$\beta_q = \left(\frac{1}{2 - u\alpha}\right)^{\frac{1}{q+1}}, \quad \text{otherwise}$$

where, $\alpha = 2 - \beta^{-(q+1)}$ and β is calculated as

$$\beta = 1 + \frac{2}{x_2 - x_1} \min[(x_1 - x_l), (x_u - x_2)]$$

Here, x_l and x_u are the lower and upper bounds on the parameter x .

3.4 Multi-objective genetic algorithm

In a classical optimization approach only a single objective function is minimized leading to a unique solution in general. Practical design problems do not look like this. Dynamic systems have to be optimized with respect to several conflicting specifications and several different designs are acceptable as optimal with respect to the same set of specifications. Multiple optimal solutions exist because no one solution can be optimal for multiple conflicting objectives. Once such multiple solutions are found, usually, a higher-level decision-making strategies is adopted to choose one solution from the set of obtained Pareto-optimal solutions.

The principles of multi-criterion optimization are different from that in a single-objective optimization. The main goal in a single- objective optimization is to find the global optimal solution. However, in a multi-criteria optimization there are more than one objective function, each of which may have a different individual optimal solution. If there is sufficient difference in the optimal solutions corresponding to different objectives, the objective functions are often known as conflicting to each other. In the present study the two conflicting objectives considered are the minimization of vertical displacement and minimization of vertical acceleration . The classical ways of tackling multi-objective optimization problems is straight forward [16, 17, 18, 23, 25]: Convert multiple objectives into one objective. There exists a number of conversion method- weighted sum approach, ϵ -perturbation method, Tchybeshev method, min-max method, goal programming method and others. Since multiple objectives are converted into one objective, the resulting solution to the single-objective optimization problem is usually subjective to the parameter settings chosen by the user. Moreover, since usually a classical optimization method is used, only one solution can be found in one simulation run. Thus, in order to find multiple Pareto-optimal solutions, the chosen optimization algorithm must have to be used a number of times.

Furthermore, the classical methods have been found to be sensitive to the convexity and continuity of the Pareto- optimal region. In this study a multi-objective genetic algorithm is used in conjunction with a numerical integration technique.

Multi-objective evolutionary algorithms with such conflicting objective functions give rise to a set of optimal solutions, instead of one optimal solution. The reason for the optimality of many solutions is that no one can be considered to be better than any other with respect to all objective functions. These optimal solutions have a special name -- Pareto-optimal solutions.

The concept of optimality in multi-criterion optimization deals with a number (or a set) of solutions, instead of one solution. Based on this, we first define conditions for a solution to become dominated with respect to another solution and then present conditions for a set of solutions to become a Pareto-optimal set.

Definition 1 *Pareto-optimal Front is the set of solutions which are equally good as compared to any other solution of the set i.e. any solution on the front can not be selected when compared with other, without being biased towards other. Mathematically it can be given as : "A decision vector $x \in X_f$ is said to be non-dominated regarded to a set $A \subseteq X_f$ if*

$$\nexists a \in A : a \succ x$$

If it is clear within the context which set A is meant, it is simply left out. Moreover, x is said to be Pareto-optimal if x is non dominated regarding X_f ."

Figure 3.4 gives a better illustration of the concept of Pareto- optimality through a example problem of trade-off between two conflicting objectives namely, cost and the accident rate, both to be minimized. The point A represents the solution with a very small cost but highly accident prone. Another solution B represents the solution very safe but very costly. Here both the solutions are good with respect to the one objective, but worse in other objective. There exist a lot of solutions (like solution D) which also belong to the Pareto-optimal set and have equal importance to a unbiased decision maker. All these solutions (lying on the thick solid line) are known as the members solutions (lying on the thick solid line) are known as the members of *Pareto-optimal Front* and this solid line is called *Pareto-optimal Front*.

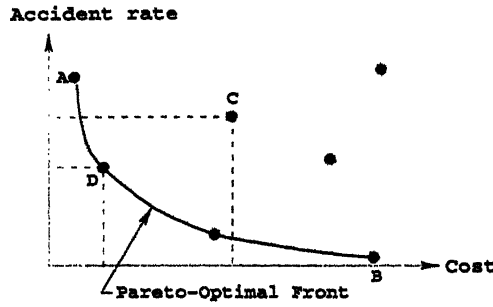


Figure 3.3: The concept of Pareto-optimal solutions is illustrated.

3.5 Dominance

This is a very important concept so far as the discussion on multi-objective problems is concerned. This forms the back bone of the ranking strategy. For constrained and unconstrained dominance definition varies. Both of the definitions are given as following.

3.5.1 Dominance for unconstrained problems

Definition 2 *If there are N objective functions and two individuals, "a" and "b" are compared then*

$$\begin{aligned}
 &a \succ b \text{ (a dominates b)} \quad \text{if } f(a) > f(b). \\
 &\quad f(a) > f(b) \text{ means that} \quad \forall i \in N \quad f_i(a) > f_i(b) \\
 &\text{or} \\
 &a \succeq b \text{ (a weakly dominates b)} \quad \text{if } f(a) \geq f(b). \\
 &\quad f(a) \geq f(b) \text{ means that} \\
 &\quad \forall i \in N \quad f_i(a) \geq f_i(b) \\
 &\quad \text{and} \quad \wedge i \in N \quad f_i(a) > f_i(b) \\
 &\text{or} \\
 &a \sim b \text{ (a is indifferent to b)} \quad \text{if } f(a) \not\geq f(b) \\
 &\quad \wedge \quad f(b) \not\geq f(a)
 \end{aligned}$$

In simple words it can be said, that "a dominates b" if and only if for all function values, the function value of a is either better or at least equal to that of function value of b , and at least one function value of a is better than b . If all function values of a are equal to those of b or if in some function values a is better and for some function values b is better, a and b are said to be *indifferent* to each other.

This can be understood with the help of the Figure 3.4. It is observed that the solutions which are not on the Pareto-optimal front (like solution C) also exists. If it is compared with solution A, according to definition 2 both are indifferent. But if it is compared with another solution D, it is found to be dominated by solution D. Since for a solution C, there exists a solution D in the search space, which dominates it, this solution can't be in Pareto-optimal Front.

3.5.2 Dominance for constrained problems

In the multi-objective cases where the constraints are present, definition of “dominance” is redefined to accommodate the constraints.

Definition 3 *The definition of dominance when more than one constraints are present is given according to the following conditions.*

Condition 1: *If individual A is feasible and individual B is not then A dominates B.*

Condition 2: *If individual B is feasible and individual A is not then B dominates A.*

Condition 3: *If both of the individuals are infeasible then the individual with lesser violation of constraint(s) dominates the other.*

Condition 4: *If both of the individuals are feasible or equally infeasible, dominance is decided according to the definition 2*

There are primarily two goals that a multi-criterion optimization algorithm must try to achieve:

- Guide the search towards the global Pareto-optimal region, and
- Maintain population diversity in the Pareto-optimal front.

3.5.3 Constraint handling

The steps for constraints handling are given as following:

1. Normalise the jerk and the frequency constraints.
2. Find the square sum of the constraint violation (if any). If none of the constraints is violated, corresponding violation is set to zero. The function is considered to be equal to sum of it's value and the square sum of the constraints multiplied by a penalty parameter. This is termed as penalty function method. However, this leads to distortion of function, so it is not preferred. In the present work we are using tournament selection scheme for the constraint handling purpose.
3. Tournament selection is done to handle the constraints as suggested by *Deb*, [20, 19]. Tournament Size taken is two. Winner of the tournament between two solutions is decided by following the constraint domination conditions.
 - *Condition 1:* If any of the individual is feasible and other is not, select the feasible individual.
 - *Condition 2:* If both individual are infeasible select the individual with least error or constraint violation.

- *Condition 3:* If both individuals are feasible or both are infeasible with same constraint violation, select the individual with better fitness.

3.6 Srinivas and Deb's non-dominated sorting genetic algorithm (NSGA)

The idea behind the NSGA [21] is that a ranking selection method is used to emphasize current non-dominated points and sharing function method is used to maintain diversity in the population. NSGA differs from a simple genetic algorithm only in the way the selection operator is used. The cross-over and mutation operators remain as usual. Before the selection is performed, two procedures are performed serially:

1. Classifying a population according to non domination. The first set of non-dominated solutions is assumed to constitute the first non-dominated front in the population. In order to find the solutions belonging to the second level of non domination, the solutions of the first level of non-domination can be temporarily disregarded. This procedure is continued till all the solutions are classified into a level of non-domination (rank).

2. Fitness assignment using sharing function: Initially the fitness is assigned to each level according to its rank. An individual in a higher level gets lower fitness. This is done in order to maintain a selection pressure for choosing solutions from lower levels of non-domination. Thus, the search is guided towards the Pareto-optimal region. To obtain diversity among the current nondominated solutions, lonely solutions are emphasized using a sharing function strategy. So the fitness assignment is done in two stages. Firstly, all the solutions in the first non-dominated front are assigned a fitness (dummy fitness) equal to the population size. Based on the sharing strategy, if a solution has many neighbouring solutions in the same front, its dummy fitness is reduced by a factor and a shared fitness is computed. This factor (usually known as niche count) depends on the number and proximity of neighbouring solutions. Thereafter, individuals in the second non-domination level are all assigned a dummy fitness equal to a number smaller than the smallest shared fitness of the previous front. Then, shared fitness values are calculated for every individual and the process is repeated.

3.7 Non-dominated sorting genetic algorithm-II (NSGA-II)

Multi-objective evolutionary algorithms which use non-dominated sorting and sharing have been mainly criticized for their

1. $O(mN^3)$ computational complexity (where m is the number of objectives and N is the population size),

2. non-elitism approach,
3. the need for specifying a sharing parameter.

NSGA-II [4] alleviates all the above three difficulties. Specifically, a fast non-dominated sorting approach with $O(mN^2)$ computational complexity is used. Second, a selection operator is presented which creates a mating pool by combining the parent and child populations and selecting the best (with respect to fitness and spread) N solutions. In the present study NSGA-II has been used for the purpose of optimization owing to low computational requirements, elitist approach, and parameter-less sharing approach. In the following we give a brief description of NSGA-II [4].

3.7.1 A fast non-dominated sorting approach

First, for each solution, two entities are calculated :

1. n_i , the number of solutions which dominate the solution i , and
2. S_i , a set of solutions which the solution i dominates.

The calculation of these two entities requires $O(mN^2)$ comparisons. We identify all those points which have $n_i = 0$ and put them in a list F_1 . F_1 is called the current front. Now, for each solution in the current front we visit each member (j) in its set S_i and reduce its n_j count by one. In doing so, if for any member j the count becomes zero, we put it in a separate list F_2 . When all the members of the current front have been checked, the members in the list F_1 are declared as members of the first front. We then continue this process using the newly identified front F_2 as our current front.

Each such iteration requires $O(N)$ computations. Since at most there can be N fronts, the worst case complexity of this loop is $O(N^2)$. The overall complexity of the algorithm now is $O(mN^2) + O(N^2)$ or $O(mN^2)$.

3.7.2 Density estimation

To get an estimate of the density of solutions surrounding a particular point in the population, we take an average distance of the two points on either side of this point along each of the objectives. This quantity $i_{distance}$ serves as an estimate of the size of the largest cuboid enclosing the point i without including any other point in the population (we call this crowding distance). In figure 3.4, the crowding distance of the i_{th} solution in its front (marked with solid circles) is the average side-length of the cuboid shown.

3.7.3 Crowded comparison operator

The crowded comparison operator (\geq_n) guides the selection process at the various stages of the algorithm towards a uniformly spread out Pareto-optimal front.

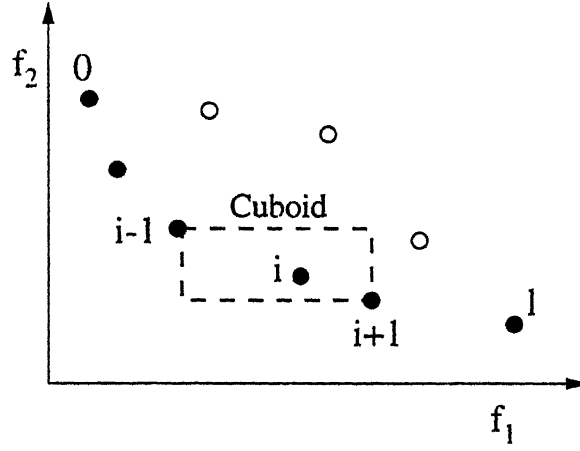


Figure 3.4: The crowding distance calculation is as shown

It is assumed that every individual 'i' in the population has two attributes.

1. Non-domination rank (i_{rank})
2. Local crowding distance ($i_{distance}$)

We now define a partial order \geq_n as :

$$i \geq_n j \text{ if } (i_{rank} < j_{rank}) \text{ or } ((i_{rank} = j_{rank}) \text{ and } (i_{distance} > j_{distance}))$$

That is, between two solutions with differing non-domination ranks we prefer the point with the lower rank. Otherwise, if both the points belong to the same front then we prefer the point which is located in a region with lesser number of points (the size of the cuboid enclosing it is larger).

3.7.4 The main loop

Initially, a random parent population P_0 is created. The population is sorted based on non-domination. Each solution is assigned a fitness equal to its non-domination level (1 is the best level). Thus, minimization of fitness is assumed. Binary tournament selection, recombination, and mutation operators are used to create a child population Q_0 of size N . From the first generation onward, the procedure is different. The elitism procedure for $t \geq 1$ and for a particular generation is shown in the following:

First, a combined population $R_t = P_t \cup Q_t$ is formed. Then the population R_t (of size $2N$) is sorted according to non-domination. The new parent population P_{t+1} is formed by adding solutions starting from the first front till the size of the next front exceeds the number of individuals (n) required to

complete the population N . Thereafter, the solutions of this front are sorted according to f_{fit} and the first n' individuals are picked. This is how we construct the population P_{t+1} of size N . This population of size N is now used for selection, cross-over, mutation to create a new population Q_{t+1} of size N .

3.8 Numerical integration algorithm

A good ordinary differential integrator should exert some adaptive control over its own progress, making frequent changes in its stepsize. Usually the purpose of this adaptive stepsize control is to achieve some predetermined accuracy in the solution with minimum computational effort. Many small steps should tiptoe through treacherous terrain, while a few great strides should speed through smooth smooth uninteresting countryside. The resulting gains in efficiency are not mere tens of percents or factors of two: they can be sometimes a factor of ten, a hundred, or more. Sometimes accuracy may be demanded not directly in the solution itself, but in some related conserved quantity that can be monitored.

Implementation of adaptive stepsize control requires that the stepping algorithm signal information about its performance, most important, an estimate of its truncation error. Obviously, the calculation of this information will add to the computational overhead, but the investment is generally repaid handsomely.

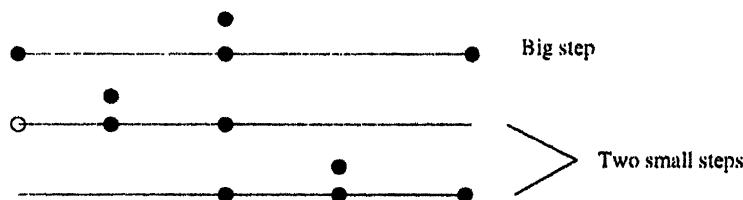


Figure 3.5: Step doubling as a means for adaptive stepsize control in 4th order Runge-Kutta : points where the derivative is evaluated are shown as filled circles. The open circle represents the same derivatives as the filled circle immediately above it, so the total number of evaluations per step is 11 per two steps.

With fourth order Runge-Kutta method, the most straightforward technique by far is step doubling [3] as shown in the figure 3.8. We take each step twice, one as a full step, then, independently as two half steps. Each of the three separate Runge-Kutta steps in the procedure requires 4 evaluations, but the single and double sequences share a starting point, so the total is 11. This is to be compared not to 4, but to 8 (the two half steps), since —stepsize control aside—we are achieving the accuracy of the smaller (half) stepsize.

If we denote the exact solution for an advance from x to $x+2h$ by $y(x+2h)$ and the two approximate

solutions be y_1 (one step $2h$) and y_2 (2 steps each of size h). Since the basic method is fourth order, the true solution and the two numerical approximation are related by

$$y(x + 2h) = y_1 + (2h)^5 \phi + O(h)^6 + \dots \quad \dots(1)$$

$$y(x + 2h) = y_2 + 2(h)^5 \phi + O(h)^6 + \dots \quad \dots(2)$$

where to order h^5 , the value ϕ remains constant over the step. [Taylor series expansion tells us the ϕ is a number whose order of magnitude is $y^{(5)}(x)/5!$.] The first equation, i.e. the equation (1) involves $(2h)^5$ since the step-size is $2h$, while the equation (2) involves $2(h)^5$ since the error on each step is $h^5 \phi$. The difference between the two numerical estimates is a convenient indicator of truncation error

$$\Delta = y_2 - y_1 \dots \dots \dots (3)$$

It is this difference that is to be kept to a desired degree of accuracy, neither too large nor too small. We do this by adjusting h .

Ignoring terms of order h^6 and higher, we can solve the two equations (1) and (2) to improve our numerical estimate of the true solution $y(x + 2h)$, namely,

$$y(x + 2h) = y_2 + \frac{\Delta}{15} + O(h)^6 \dots \dots (4)$$

This estimate is accurate to fifth order, one order higher than the original Runge-Kutta steps. However higher order is not always higher accuracy

An alternative step-size adjustment algorithm is based on the **embedded Runge-Kutta formulas**, originally invented by Fehlberg [3]. The general form of a fifth-order Runge-Kutta formula is

$$\begin{aligned} k_1 &= hf(x_n, y_n) \\ k_2 &= hf(x_n + a_2h, y_n + b_{21}k_1) \\ &\dots\dots\dots \\ k_6 &= hf(x_n + a_6h, y_n + b_{61}k_1 + \dots + b_{65}k_5) \\ y_{n+1} &= y_n + c_1k_1 + c_2k_2 + c_3k_3 + c_4k_4 + c_5k_5 + c_6k_6 + O(h^6) \end{aligned} \quad \dots(5)$$

The embedded fourth order formula is

$$y_{n+1}^* = y_n + c_1^*k_1 + c_2^*k_2 + c_3^*k_3 + c_4^*k_4 + c_5^*k_5 + c_6^*k_6 + O(h^5) \quad \dots(6)$$

and so the error estimate is

$$\delta = y_{n+1} - y_{n+1}^* = \sum_{i=1}^6 (c_i - c_i^*) k_i \quad ..(7)$$

The particular values of the various constants were found by Cash and Carp [3]. These give a more efficient method than Fehlberg's original values, with somewhat better error properties.

When we know, at least approximately, what our error is, we need to keep it within desired bounds. If we take a step h_1 and produce an error Δ_1 , therefore, the step h_o that would have given some other value is readily estimated as

$$h_o = h_1 \frac{|\Delta_o|^{0.2}}{|\Delta_1|} \quad ...(8)$$

Henceforth, Δ_o denotes the desired accuracy. If Δ_1 is larger than Δ_o in magnitude, the equation tells us how much to decrease the step-size when we retry the present (failed) step. If Δ_1 is smaller than Δ_o , then the equation tells us how much we can safely increase the step-size for the next step. Furthermore, because our estimates of error are not exact, but only accurate to the leading order in h , we are advised to put in a safety factor S which is a few percent smaller than unity.

$$h_o = Sh_1 \left(\frac{|\Delta_o|}{|\Delta_1|} \right)^{0.20} \quad \Delta_o \geq \Delta_1$$

$$h_o = Sh_1 \left(\frac{|\Delta_o|}{|\Delta_1|} \right)^{0.25} \quad \Delta_o < \Delta_1$$

This prescription is found to be a a reliable one in practice.

3.9 GA in conjunction with numerical integration algorithm

The numerical integration algorithm works in conjunction with the genetic algorithm used. Initially, the GA which may be RGA or NSGA-II, sets a random population of design variables. The limits of these variables is supplied to th GA code. Then every set of design variables value is sent to the numerical integration algorithm which computes the vehicle's dynamic response, i.e., the displacements and accelerations and then transfers their maximum values back to the genetic algorithm . The genetic algorithm then assigns a fitness after considering the constraint violations. Then the second set of design variables

is sent to the numerical integration algorithm. Thus, the fitness of whole set of initial population is determined. Then the selection, cross-over and mutation operators operate on the population and form a new population. This population again goes through the same process. Thus, after a number of such generations the optimal results are obtained. The step by step procedure for the whole of the algorithm is as follows :

Step 1: Initialize the population.

Step 2: For every individual of this random population, the adaptive step-size control Runge-Kutta method, calculates the dynamic response for the whole period of travel for different sets of excitation functions. The initial values of both the displacement and velocity are fixed as zero.

Step 3: The maximum values for the displacement, acceleration and jerk are calculated. Then the different frequencies are calculated, and their maximum and minimum values are found.

Step 4: Calculate the objective function values as obtained from the numerical integration algorithm.

Step 5: Rank the population using the dominance definition defined in Section 3.5 as applicable for non-dominated sorting [21].

Step 6: Calculate the crowding distance [Section 3.7.3].

Step 7: Do selection using crowding comparison operator [Section 3.7.4].

Step 8: Do crossover, mutation and generate the intermediate children population.

Step 9: Combine the intermediate population and parent population and do non-dominated sorting and find crowding distance.

Step 10: New parent population is formed by accepting solutions from the first (best) non-dominated front and continuing to other fronts successively till the new population exceeds the number of individuals as the parent population had.

tep 11: The solutions from the last accepted front are sorted according to the crowding distance and as many individuals are selected, which make the population of new parent population same as old one.

tep 12: Repeat Step 2.

3.10 Closure

This chapter includes the study of various algorithms that have been used in the present work. We start with simple genetic algorithm and then move on to the real-coded genetic algorithm. After single objective optimization using GAs we proceed to multi-objective genetic algorithms. A brief description of various features of these algorithms is also presented. We also study an effective constraint handling technique used in genetic algorithms. Then we present NSGA-II algorithm that has been used in the present study. In the end we discuss the adaptive step-size control Runge-Kutta method which has been used in conjunction with the NSGA-II algorithm.

Chapter 4

Car suspension models

4.1 Two dimensional model

In a two dimensional model of a car suspension system only two wheels (one each at rear and front) are considered. Thus, the sprung mass is considered to have vertical and pitching motions only. No rolling motion of the car can be considered in this model. Side to side suspension interactions will be neglected. They are of course a major factor in cornering behaviour, but the phenomena of bouncing and pitching are experienced in the main when travelling in a straight line. Both the front and the rear wheels go through the same road ridge. The two dimensional model is shown in the figure 4.1 The two dimensional model is better approximation than the quarter model in the sense that the pitching motion can also be considered and since the rear wheel is included, the wheelbase filtering effect is also present in the response obtained

4.1.1 Design variables and system constants

In order to formulate the optimal design problem the first task is to identify the important design variables. Let us first identify all design parameters that govern the dynamic behaviour of the car vibration :

- Sprung mass, m_s
- Front unsprung mass, m_{fu}
- Rear unsprung mass, m_{ru}
- Front coil stiffness, k_{fs}
- Rear coil stiffness, k_{rs}
- Front damper coefficient, c_f
- Rear damper coefficient, c_r

- Front tyre stiffness, k_{ft}
- Rear tyre stiffness, k_{rt}
- Axle to Axle distance, L
- Moment of inertia for pitching, J_p

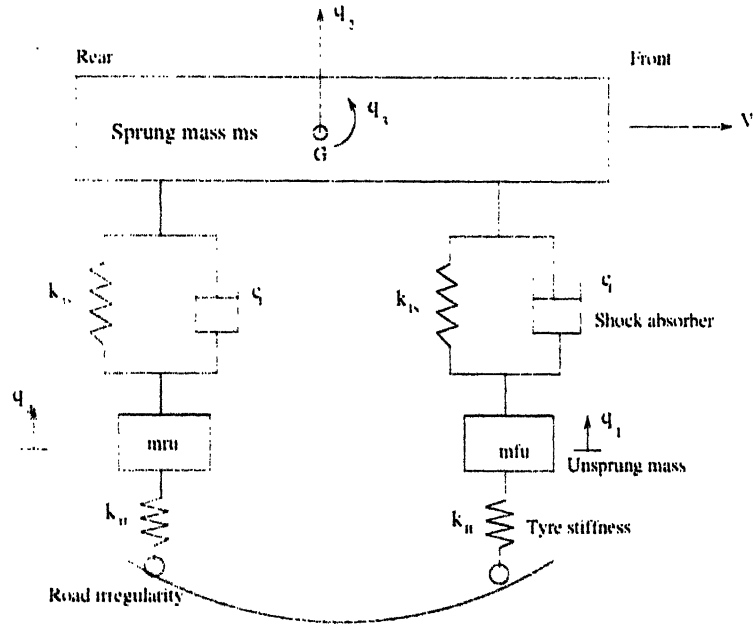


Figure 4.1: The dynamic model of the car suspension system, The above model has four degrees of freedom

Since a suspension designer is interested in choosing the optimal dampers and suspension coils, we consider only four of the above parameters, front coil stiffness k_{fs} , rear coil stiffness k_{rs} , front damper coefficient c_f , rear damper coefficient c_r -- as design variables.

Also, most suspension coils and dampers used in cars have nonlinear characteristics. The spring rate or the damping coefficient does not remain constant for all displacement or velocities. They are usually found to vary in a piecewise linear form as shown for the rear suspension coil in figure 4.2. For simplicity, we consider k_{rs}^a (when the deflection is between zero and a value δ) as the variable and other two spring rates, k_{rs}^b (when the deflection is more than δ) and k_{rs}^c (when the deflection is negative); as to vary in a fixed proportion with respect to k_{rs}^a . Dampers at front and rear are also considered to vary in a similar fashion. However, the front suspension spring is assumed to vary linearly, as commonly followed in automobile industries.

Following values are obtained from one automobile manufacturer :

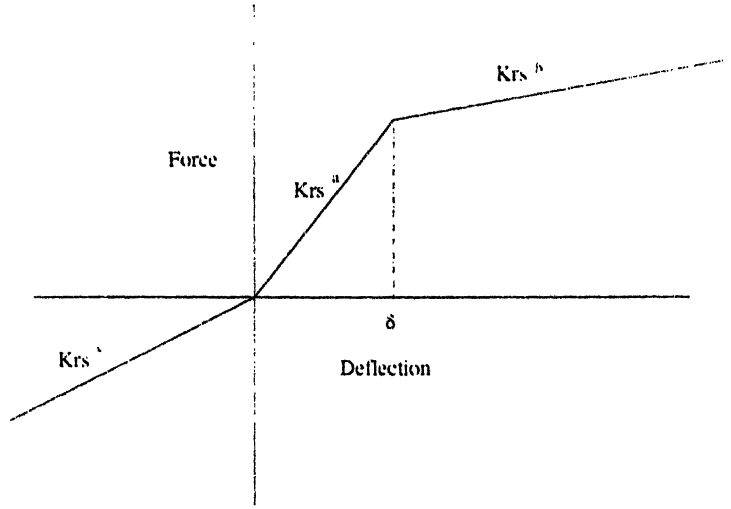


Figure 4.2: Bilinear variation of rear suspension stiffness with deflection

- $k_{rs}^b/k_{rs}^a = 1.28$
- $c_f^b/c_f^a = 0.033$
- $c_r^b/c_r^a = 0.257$
- $k_{rs}^c/k_{rs}^a = c_f^c/c_f^a = c_r^c/c_r^a = 1$
- $\delta_{ks} = 215 \text{ mm}$, $\delta_{cf} = 50 \text{ mm/s}$, and $\delta_{cr} = 100 \text{ mm/s}$.

4.1.2 Mathematical modelling

Modelling requires several steps of mechanical and mathematical idealization. In the multi-body system approach, deformations of the bodies are neglected and the bodies are considered rigid. They are connected by ideal links and bearings allowing some well defined motion of the bodies relative to each other. Coupling elements like springs and dampers determine the dynamics of the systems.

The dynamic behaviour for the two dimensional model in steady state vibration can be obtained by writing Newton's Second law for the sprung and unsprung masses. By drawing a Free body diagram for each, and considering the forces acting on the sprung mass and on the front and rear unsprung mass, we write the differential equations governing the vertical motion of the unsprung mass at the front axle (q_1), the sprung mass (q_2), and the unsprung mass at the rear axle (q_4), and the angular motion of the sprung mass (q_3) as follows (Deb, 1995) :

$$\ddot{q}_1 = (F_2 + F_3 - F_1)/m_{fu} \quad (4.1)$$

$$\ddot{q}_2 = -(F_2 + F_3 + F_4 + F_5)/m_s \quad (4.2)$$

$$\ddot{q}_3 = [(F_4 + F_5)l_2 - (F_2 + F_3)l_1]/J_p \quad (4.3)$$

$$\ddot{q}_4 = (F_4 + F_5 - F_6)/m_{ru} \quad (4.4)$$

The parameters l_1 and l_2 are the horizontal distances of the front and rear axle from the center of gravity of the sprung mass. Forces F_1 to F_6 are calculated as follows :

$$F_1 = k_{f1}d_1, \quad F_2 = k_{fs}d_2, \quad F_3 = c_f\dot{d}_2,$$

$$F_4 = k_{rs}d_1, \quad F_5 = c_r\dot{d}_4, \quad F_6 = k_{rs}d_3.$$

The parameters d_1 , d_2 , d_3 and d_4 are the relative deformations in the front tyre, the front spring, the rear tyre, and the rear spring, respectively. The parameters \dot{d}_2 and \dot{d}_4 are relative velocities in the front and rear dampers, respectively. Figure 4.1 shows all the four degrees-of-freedom of the above system (q_1 to q_4). The relative deformations in springs and tyres can be written as follows :

$$d_1 = q_1 - f_1(t),$$

$$d_2 = q_2 + l_1q_3 - q_1,$$

$$d_3 = q_1 - f_2(t),$$

$$d_4 = q_2 - l_2q_3 - q_4.$$

The functions $f_1(t)$ and $f_2(t)$ are road excitations as functions of time in the front and rear tyre, respectively. Any suitable road profile can be tested using these functions. For example, a bump can be modelled as $f_1(t) = A \sin(\pi t/T)$, where A is the amplitude of the bump and T the time required to cross the bump. When a car is moving forward, the front wheel experiences the bump first, while the rear wheel experiences the same bump a little later, depending on the axle-to-axle distance, L , and the speed of the car V . Thus, the function $f_2(t) = f_1(t - L/V)$. The sinusoidal bump profile with a width of 500 mm and height 70 mm is shown in the figure 4.3

The various system constants that are supplied as data to the algorithm are the front and rear unsprung masses, the sprung mass, the wheel to wheel distance, the distances of the center of gravity

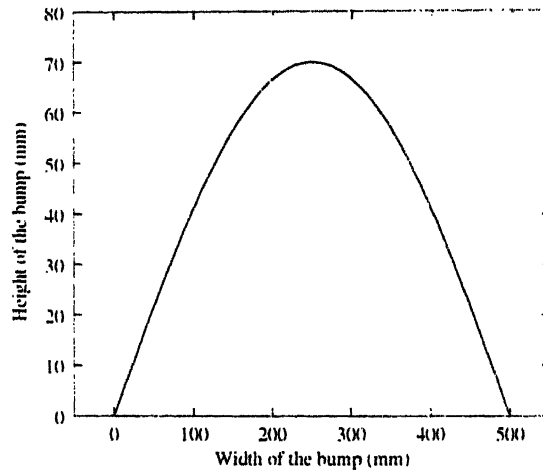


Figure 4.3: A sinusoidal bump profile

from the front and rear axle, the front and the rear tyre stiffnesses, the car speed, the width and the amplitude of the bump. These data have been obtained from a car manufacturer.

4.1.3 Objective function

The two dimensional model is first optimized using a single objective real coded GA. The objective here is to minimize the maximum transmissibility of the suspension system, i.e., the ratio of response amplitude to the excitation amplitude. The response amplitude in this case is for both pitching and bounce motion. This optimization is done subject to only one constraint, i.e., jerk constraint. A very important feature of this optimization is that we are formulating the objective function in two ways, in the first case we minimize the transmissibility only for the period when the car is not on the bump, i.e., exclude the time when any one wheel of the car is on the bump. In the second case the transmissibility is minimized for whole of the period.

However, as single objective optimization considers only one objective from a set of objectives, and overlooks the others, the optimal results obtained are very often not too good from a practical point of view. The next step of optimization is multi-objective optimization. Two conflicting objectives, i.e., minimizing the maximum transmissibility and minimizing the maximum acceleration are considered subject to only one constraint, i.e., jerk constraint. The optimization run provides us with a set of optimal solutions with a reasonable trade off. The designer can choose any of these solutions according to specific requirements.

4.1.4 Constraints and variable bounds

In the two dimensional model only one constraint is considered, i.e., jerk constraint. The optimal design must not violate this constraint. The constraint specifies the jerk (the rate of change of vertical acceleration) to be less than 18 m/s^3 (as suggested by an automobile manufacturer). The vertical jerk can be computed by numerically differentiating the vertical acceleration of the sprung mass \ddot{q}_2 .

Another important constraint is the restriction on the rattle space. It would be nice to have as soft a suspension as possible. That means lower stiffness values but this may lead to crushing of the car parts between the axle and the chassis. So there must be a minimum rattle space constraint. Also, a softer suspension leads to problem in the handling of car, so from the safety point of view it is imperative that the suspension is not too soft. However, these things can also be handled by putting a lower bound on the stiffness and damping coefficients. So, we have used some lower and upper bounds for the design variables.

4.1.5 Algorithm used

For the multi-objective optimization, a multi-objective algorithm, by the name of Non dominated sorting genetic algorithm -II (NSGA-II) [4] is used in conjunction with a numerical integration technique. The coupled differential equations specified in equations (4.1) to (4.4) are solved using adaptive step-size control Runge-Kutta fourth order algorithm. The numerical integration routine finds the dynamic response of the suspension system to the road excitation for a set of design variable values provided by the genetic algorithm and returns back the maximum transmissibility and maximum acceleration values which become the two objectives for the multi-objective algorithm.

In the case of single objective optimization, a real coded GA with Simulated binary cross-over is used in conjunction with the numerical integration technique. The real coded GA works in the real space so more accurate results are obtained.

4.2 Three dimensional model

In the three dimensional model, all four wheels are considered. Thus, the rolling motion of the sprung mass can also be studied. The sprung mass can have three motions—vertical bouncing, pitching, and rolling. Besides, each of the four unsprung masses will have a vertical motion. Thus, there are a total of seven second-order differential equations governing the motion of the sprung and the unsprung masses.

4.2.1 Design variables and system constants

Since both left and right rear (or front) wheels have the same suspension system, the number of design variables in the three dimensional optimal design model is also four. However, the dynamics of the car will be different from that in the two dimensional case. Also, there are two more system constants besides the system constants that are present in the two dimensional model, namely:

- Moment of inertia for rolling, J_r .
- Distance between the left and right wheels, l_r .

In 3-D model also, the bilinearity of the dampers and the rear springs are considered. They vary in a piecewise linear fashion similar to that in the 2-D model. However, we consider the modified values of the left and the right suspension separately as the displacement and velocity values for the two vary differently. The limits on the value of deformation and the rate of deformation in the springs and the dampers respectively are the same as used in the 2-D model.

4.2.2 Mathematical modelling

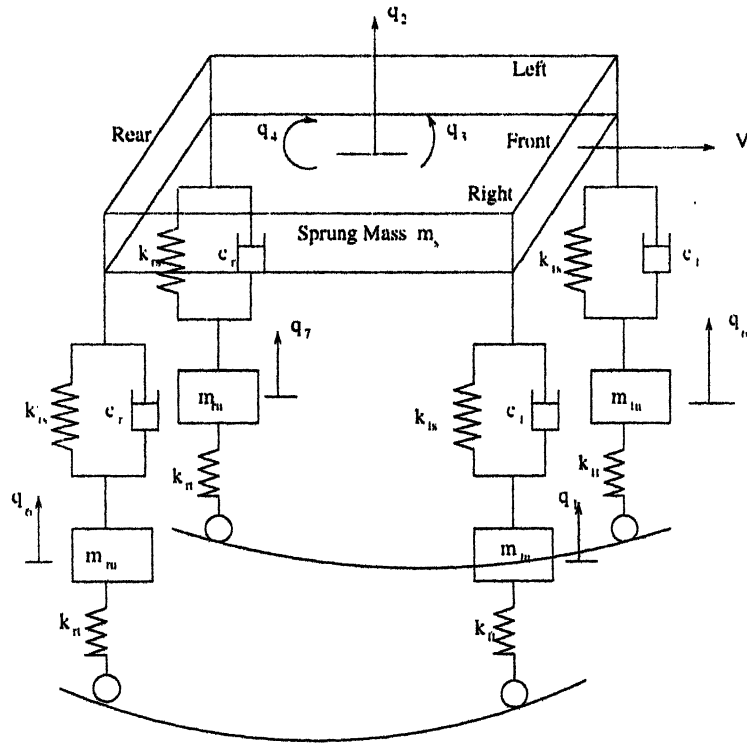


Figure 4.4: A dynamic car suspension model with seven degrees of freedom

In the 3-D model as shown in figure 4.4 there are a total of seven second order differential equations which are derived using Newton's second law for the sprung and the unsprung masses. By drawing a free body diagram for each, and considering the forces acting on the sprung mass and on the front and rear unsprung mass, we write the differential equations, for the vertical motion of the unsprung masses at the right side and the left side on the front axle (q_1 and q_6 respectively), the vertical motion of the sprung mass (q_2), the vertical motion of the unsprung masses at the right side and the left side on the rear axle (q_5 and q_7 respectively) and the pitching and rolling motions of the sprung mass (q_3 and q_4 respectively). The equations are as follows :

$$\ddot{q}_1 = (F_2 + F_3 - F_1)/m_{fu} \quad (4.5)$$

$$\ddot{q}_2 = -(F_2 + F_3 + F_4 + F_5 + F_8 + F_9 + F_{10} + F_{11})/m_s \quad (4.6)$$

$$\ddot{q}_3 = [(F_4 + F_5 + F_{10} + F_{11})l_2 - (F_2 + F_3 + F_8 + F_9)l_1]/J_p \quad (4.7)$$

$$\ddot{q}_4 = [(F_8 + F_9 + F_{10} + F_{11}) - (F_2 + F_3 + F_4 + F_5)]l_r/J_r \quad (4.8)$$

$$\ddot{q}_5 = (F_4 + F_5 - F_6)/m_{ru} \quad (4.9)$$

$$\ddot{q}_6 = (F_8 + F_9 - F_7)/m_{fu} \quad (4.10)$$

$$\ddot{q}_7 = (F_{10} + F_{11} - F_{12})/m_{ru} \quad (4.11)$$

The forces F_1 to F_{12} are calculated as follows:

$$F_1 = k_{fl}d_1, \quad F_2 = k_{fs}d_2, \quad F_3 = c_f\dot{d}_2, \quad F_4 = k_{rs}d_4,$$

$$F_5 = c_r\dot{d}_4, \quad F_6 = k_{rt}d_3, \quad F_7 = k_{ft}d_5, \quad F_8 = k_{fs}d_6,$$

$$F_9 = c_f\dot{d}_6, \quad F_{10} = k_{rs}d_8, \quad F_{11} = c_r\dot{d}_8, \quad F_{12} = k_{rt}d_7.$$

The parameters d_1 , d_2 , d_3 and d_4 are the relative deformations in the front right tyre, front right spring, rear right tyre and the rear right spring respectively. The parameters d_5 , d_6 , d_7 , d_8 are the relative deformations in the front left tyre, front left spring, rear left tyre and rear left spring respectively.

The parameters \dot{d}_2 , \dot{d}_4 , \dot{d}_6 and \dot{d}_8 are the relative velocities in the front right damper, rear right damper, front left damper and rear left damper respectively. The relative deformations in the springs and the tyres can be written as follows :

$$d_1 = q_1 - f_1(t),$$

$$d_2 = q_2 + l_1 q_3 + l_r q_1 - q_1,$$

$$d_3 = q_5 - f_2(t),$$

$$d_4 = q_2 + l_2 q_3 + l_r q_1 - q_5,$$

$$d_5 = q_6 - f_1(t),$$

$$d_6 = q_2 + l_1 q_3 + l_r q_1 - q_6,$$

$$d_7 = q_7 - f_2(t),$$

$$d_8 = q_2 + l_2 q_3 + l_r q_1 - q_7$$

The functions $f_1(t)$ and $f_2(t)$ are road excitations as functions of time in the front and rear tyre, respectively. The road profile that was tested in the two dimensional case was a sinusoidal profile. In the three dimensional case different excitation functions used are as follows :

1. A bump modelled as $f_1(t) = A[1 - \cos(2\pi t/T)]/2$, where A is the amplitude of the bump and T the time required to cross the bump. The rear wheel experiences the same bump a little later, depending on the wheel to wheel distance and the car speed. Thus, the function $f_2(t) = f_1(t - L/V)$. A bump of this profile having a width of 2000 mm and height of 70 mm is shown in figure 4.5. It is to be noted that the same kind of excitation is experienced by the right and the left tyres and we ignore the lateral interaction between the right and left suspensions.
2. Three similar bumps equally spaced having the same profile as in the above case. The gap between the bumps is taken as equal to the width of the bump. The bumps in series are shown in the

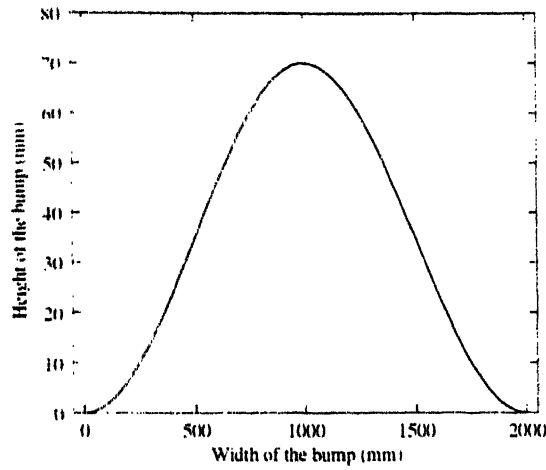


Figure 4.5: Single bump profile

figure 4.6.

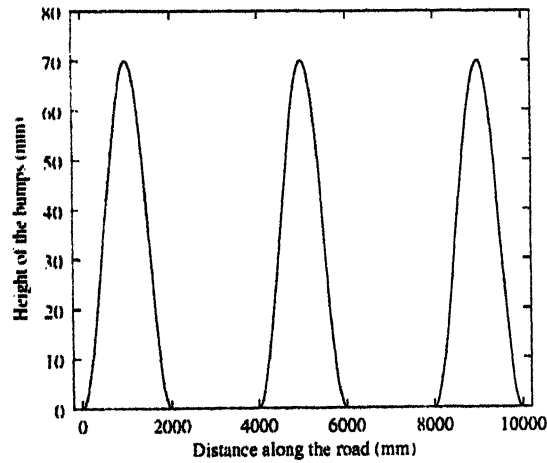


Figure 4.6: Three bumps in series

3. A rounded displacement step function as follows [15]:

$f_1(t) = A[1 - (1 + \gamma T)e^{(-\gamma T)}]$ where A is the amplitude of the displacement step and T is the non-dimensionalised time, i.e., $T = t/(L/V)$ and γ is the severity parameter for shock excitation. This kind of base excitation with γ equal to 0.1 and 50 is shown in the figure 4.7. This type of step function is used to see the effect of non-linear damping. For the rolling motion, we have considered a rounded pot-hole which has the same mathematical expression as above, but with a negative sign.

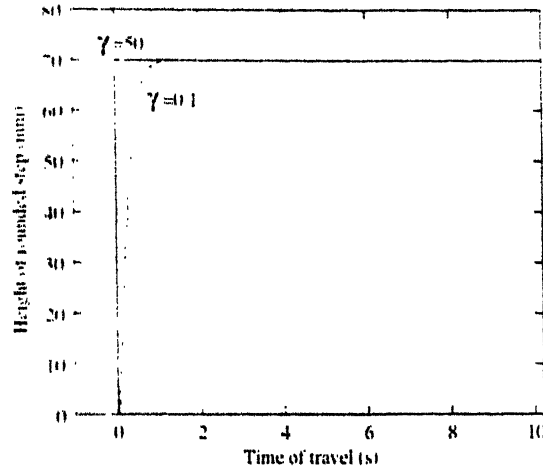


Figure 4.7: Rounded displacement step function

4.2.3 Objective function

Firstly, real coded GA is used to optimize a single objective, which is considered to be the vertical transmissibility, in the case of vertical bounce motion.

In the case of pitching and rolling motions the single objective considered is pitching and rolling amplitudes of the sprung mass respectively. In the case of 3-D model we consider only the case in which the whole time of travel is considered, as in the case of transient response it is more important to minimize the maximum values of displacement and acceleration even if it comes at the cost of little ride comfort.

After the single objective optimization multi-objective optimization is performed by considering two conflicting objectives which are of importance to the suspension designer. The suspension system is subjected to all the above four set of excitation functions to study the performance of the suspension characteristics to the different road profiles and to understand, the control that has to be exercised on the different design variables in order to obtain a suspension system that is good for a wide range of road excitations. The various conflicting objectives that have been considered for the purpose of multi-objective optimization are as follows :

1. The vertical bounce motion and the vertical acceleration. We have considered the vertical transmissibility in place of vertical displacement. The transmissibility is given by q_2^{max}/A .
2. The pitching amplitude and the pitching acceleration.
3. The rolling amplitude and the rolling acceleration. However, the rolling motion has been considered in the case of the rounded displacement step kind of function only. It is used to represent

one set of wheels (right or left) falling in a pot-hole which are so commonly found on the roads.

4.2.4 Constraints

In the two dimensional model only the jerk constraint was considered. In the three dimensional model there are five constraints which are considered. The optimal design must not violate any of these constraints. The constraints are enumerated below :

1. The vertical jerk must not exceed 18 m/s^3 . The vertical jerk is calculated by numerically differentiating the vertical acceleration of the sprung mass \ddot{q}_2 . Mathematically, it is expressed as:

$$\frac{d\ddot{q}_2}{dt}^{max} < 18$$

This constraint is included for the ride comfort consideration.

2. The maximum of the front, rear and pitching frequencies should not exceed 2.5 Hz . The higher the frequencies the more uncomfortable the ride. The lower accelerations occur at lower natural frequencies. So the car suspension should not have very high values of frequencies as they lead to higher acceleration values. Mathematically, it can be expressed as

$$Fr_{max} < 2.5$$

3. The minimum of the front, rear, and the pitching frequencies should be greater than 0.8 Hz . The lower frequencies lead to more ride comfort, but they are obtained by using softer suspensions which are not so good from the ride control point of view. So a lower bound is fixed for the frequencies to have better ride control. Mathematically, it is expressed as :

$$Fr_{min} > 0.8$$

4. Also the front natural frequency should be at least 10 percent less than the rear natural frequency. This is done to make the pitching motion die faster. This may lead to longer bounce motion but vertical bounce is less annoying as compared to the pitching motion.

$$k_{fs}^a > 1.1K_{fs}$$

5. Another important constraint is the constraint on the maximum value of acceleration. This is especially important in the case of multi-objective optimization as in the optimal results certain acceleration values exceed 9.8 m/s^2 (which is the numerical value of acceleration due to gravity, i.e. ' g '). Since at such acceleration values the passenger will lose contact of his seat, such values

are useless. In the present study a constraint restricting the maximum acceleration value to 9.0 m/s^2 is used. Mathematically, the constraint is written as :

$$\ddot{q}_2^{max} < 9.0$$

Besides, these constraints, the variable bounds are also fixed in order to account for other constraints. The minimum rattle space constraint is considered by putting a lower bound on the stiffness values. This also takes care of the better ride handling aspects which are a must for the ride safety.

4.2.5 Non-linearity in damping parameters

In the 3-D model, the dampers with cubic non-linear damping are considered [6], when the road profile is modelled as a rounded displacement step. The linear model is usually considered for mathematical simplicity but in case the transient displacements are sufficiently large, then the non-linearity in the springs and the dampers cannot be ignored. The non-linearity in the damping rather than that in stiffness has a more pronounced effect on different indices expressing the performance of a suspension system. So, in the present study we have considered cubic non-linear damping in addition to linear damping, while only linear stiffness characteristics are considered throughout. In the present work we have taken a negative damping coefficient which has a numerical value equal to one-fourth of the value of linear damping coefficient.

4.2.6 Mathematical formulae used

The pitching and the rolling moments of inertia are calculated as follows:

- Polar moment of inertia

$$J_p = m_f l_1^2 + m_r l_2^2$$

- Rolling moment of inertia

$$J_r = (m_f + m_r) l_r^2$$

For the above formulae of moments of inertia, m_f and m_r are the front and rear sprung masses.

The calculation of the front and the rear natural frequencies depends on the center of gravity and spring center of the car and other parameters of the car suspension system and is derived elsewhere [2]. The front (F_f) and rear (F_r) natural frequency and the pitching natural frequency (F_p) are given as follows :

$$F_f = \frac{1}{2\pi} \sqrt{\frac{2k_{fs}(a+s-x)^2 + 2k_{rs}^a(s-b-x)^2}{m_s(K^2 + s^2)}}.$$

$$F_r = \frac{1}{2\pi} \sqrt{\frac{2k_{fs}(a-r-x)^2 + 2k_{rs}^a(r+b+x)^2}{m_s(K^2 + r^2)}}.$$

$$F_p = \frac{1}{2\pi} \sqrt{\frac{2k_{fs}(a-x)^2 + 2k_{rs}^a(b+x)^2}{m_s K^2}}.$$

where r is the distance between the center of gravity and the spring center, a and b are the distances of the spring center from front and rear wheels :

$$a = \frac{k_{rs}^a}{k_{rs}^a + k_{fs}} L,$$

$$b = \frac{k_{fs}}{k_{rs}^a + k_{fs}} L,$$

The parameters r and s are the distances of the front and the rear conjugate points from the spring center given as follows :

$$r = \frac{K^2 - x^2 - ab}{2x} - \frac{\sqrt{(K^2 - x^2 - ab)^2 + 4K^2 x^2}}{2x},$$

$$s = \frac{K^2}{r}.$$

and K is the radius of gyration about the center of gravity.

4.2.7 Nondimensionalization of the differential equations

Since we are using the adaptive step-size control Runge-Kutta method, we must guard against the step-size becoming too small, otherwise the routine will make the apparent error zero and chug happily along taking infinitely many steps and never changing the dependent variables one iota. This may specially happen at higher values of speed. Non-dimensionalisation of the equation helps to avoid this. In the three dimensional case, the differential equations were non-dimensionalised. For illustration a few of the equations are written below and their non-dimensionalised forms are also written alongwith. All the non-dimensional terms are written as capital letters.

$$T = \frac{t}{L/V},$$

$$\frac{d_1}{A} = \frac{q_1}{A} - \frac{f_1(t)}{A},$$

$$D_1 = Q_1 - F_1(t),$$

$$\frac{d_2}{A} = \frac{q_2}{A} + \frac{l_1 q_3}{A} + \frac{l_r q_4}{A} - \frac{q_1}{A},$$

$$D_2 = Q_2 + \frac{l_1}{A} Q_3 + \frac{l_r}{A} Q_4 - Q_1,$$

$$\frac{\dot{d}_2}{A} = \frac{\dot{q}_2}{A} + \frac{l_1 \dot{q}_3}{A} + \frac{l_r \dot{q}_4}{A} - \frac{\dot{q}_1}{A},$$

$$\dot{D}_2 = \dot{Q}_2 + \frac{l_1}{A} \dot{Q}_3 + \frac{l_r}{a} \dot{Q}_4 - \dot{Q}_1,$$

An example of the non-dimensionalised form of differential equation is given alongwith the original differential equation. Again the non-dimensionalised terms are in capital letters.

$$\ddot{q}_1 = (k_{fs} d_2 + c_f \dot{d}_2 - k_{ft} d_1) / m_{fu},$$

$$\ddot{Q}_1 = \frac{k_{fs}L^2}{V^2m_{fu}}D_2 + \frac{c_fL}{Vm_{fu}}\dot{D}_2 - \frac{k_{ft}L^2}{m_{fu}V^2}D_1$$

This way all the differential equations are non-dimensionalised and used in the numerical integration routine. The non-dimensionalisation helps in proper working of the routine even for higher values of the car speed.

4.3 Closure

This chapter includes the discussion on two and three dimensional models. Mathematical modelling is presented and the problem formulation is presented for both the cases, i.e. the objective function and the constraints are defined. In the three dimensional case, a discussion on nonlinearity of dampers has been included. The non-dimensionalisation of equations in the 3-D case has been discussed in the end.

Chapter 5

Results and Discussion

The single-objective optimization and the multi-objective optimization are performed on the two and three dimensional models and the results obtained are qualitatively studied.

5.1 Two dimensional model

The following parameter values are used in all simulations:

$$\begin{aligned} m_s &= 730 \text{ kg}, & m_{fu} &= 50 \text{ kg}, \\ m_{ru} &= 115 \text{ kg}, & k_{ft} &= 15 \text{ kg/mm}, \\ k_{rt} &= 17 \text{ kg/mm}, & l_1 &= 1.50 \text{ m}, \\ l_2 &= 1.35 \text{ m}, & L &= 2.85 \text{ m}, \\ V &= 5 \text{ km/hr}, & J_p &= 2.89(10^9) \text{ kg.mm}^2 \end{aligned}$$

The car motion is simulated over a *sinusoidal bump* having 500 mm width and 70 mm height. In all solutions, the spring rates are expressed in kg/mm and damping coefficients are in kg.s/mm. The variable bounds for the stiffness values are 0.50 to 8.0, while those for the damping coefficients are 0.10 to 8.0. We start by presenting the single objective (RGA) results for the two dimensional model and then follow it by the results of multi-objective optimization.

5.1.1 Single objective optimization results

The real-coded GA is used for single objective optimization. The various parameter values are as follows :

Population size : 100
 Cross-over probability : 0.85
 Mutation probability : 0.25
 X-over distribution index : 20
 Mutation distribution index : 100
 Number of generations : 200

Results with bump time excluded

In the single objective optimization results we have considered two cases in which the objective function is evaluated differently. In first case the objective function i.e. the vertical transmissibility is considered only for that part of car travel when none of the wheels is on the bump. In second case, we consider the whole time of travel, for the evaluation of the objective function. In both the cases the objective function is subjected to only one constraint, i.e. the jerk constraint. We will first present the results for the former case.

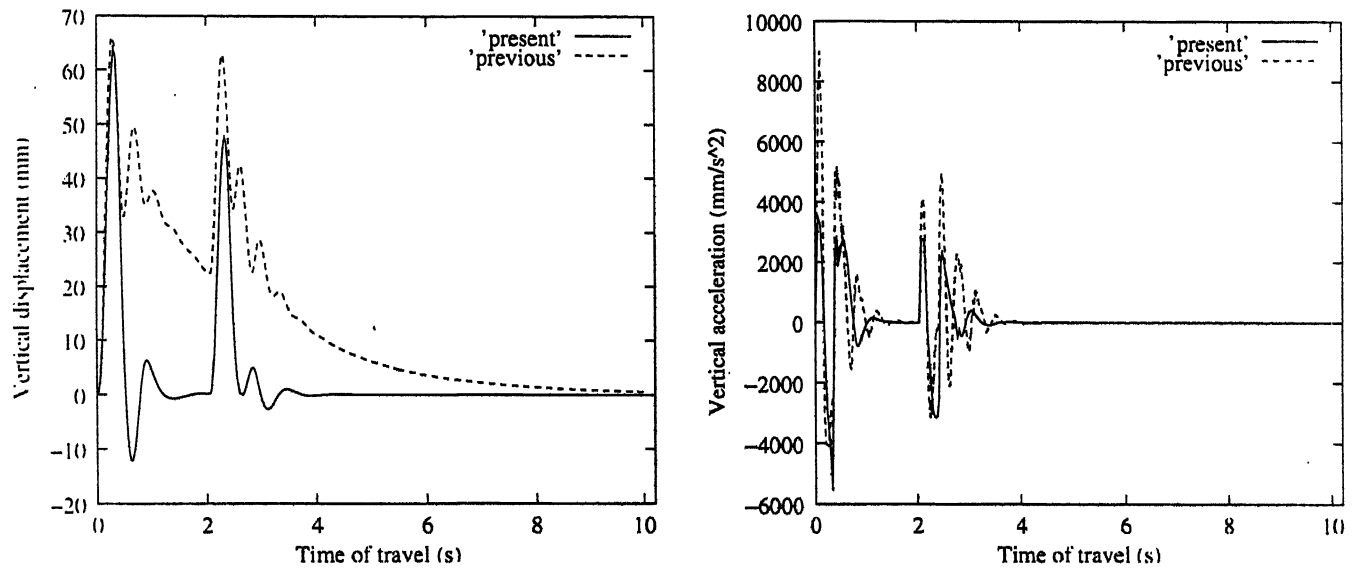


Figure 5.1: Comparison of present and previous results for the case in which the bump time is excluded.

Results	k_{fs}	c_f^a	k_{rs}^a	c_r^a	Transmissibility
Present	5.73	0.73	3.26	0.50	0.66
Previous (TELCO)	1.56	3.30	1.45	1.00	0.77

Table 5.1: Comparison of optimal values of stiffness and damping parameters for the case in which bump time is included.

The results marked as present are obtained in the present study , while the previous results are that used by an automobile manufacturer. It can be clearly seen from figure 5.1 that the present results are better in terms of both the displacement and acceleration. The optimum values of stiffness and damping parameters are given in the table 5.1. The maximum vertical jerk as calculated for the present study is 17.9 m/s^3 which makes the jerk constraint an active constraint, and indicates that the obtained result is the global optimum.

Also, we will compare the results obtained in the present work (using RGA) with those obtained by using binary coded GA (SGA) which are presented in M.Tech thesis of Mr. Vikas Saxena [1]. A comparison of results with binary coded GA is presented below.

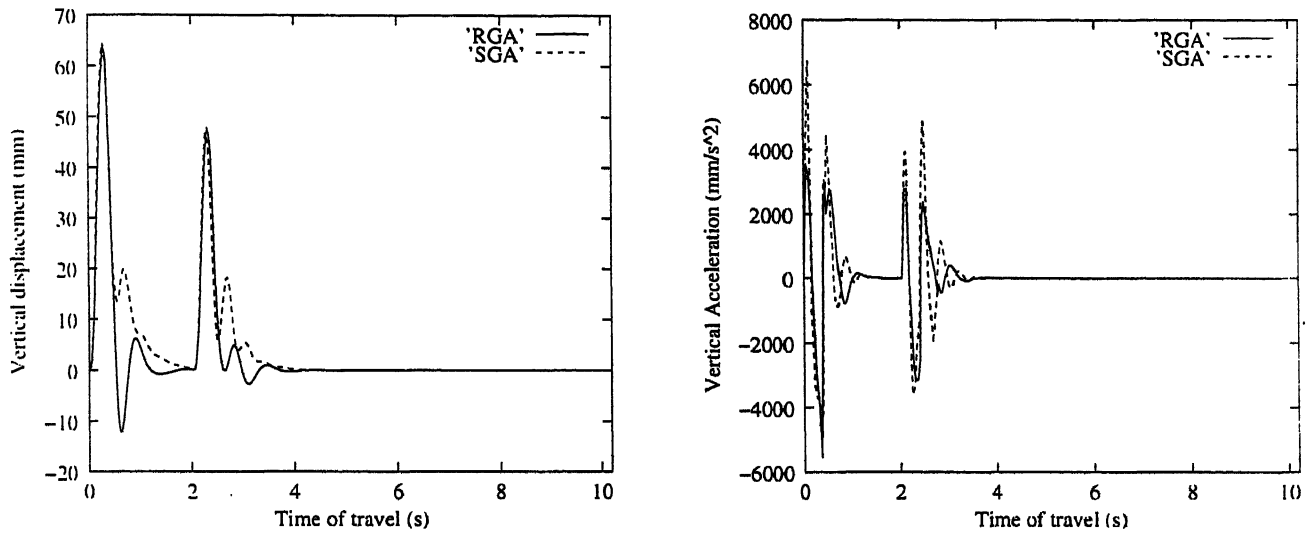


Figure 5.2: Comparison of real-coded GA and binary-coded GA results

Results	k_{fs}	c_f^a	k_{rs}^a	c_r^a	Transmissibility
RGA	5.73	0.73	3.26	0.50	0.66
SGA [1]	4.53	1.72	2.86	1.01	0.71

Table 5.2: Comparison of optimal values of stiffness and damping parameters obtained by using RGA and SGA .

It can be seen from the figure 5.2 that the results obtained using RGA are slightly better than those obtained previously by using simple genetic algorithm with binary coding. Both the displacement and acceleration responses are better in the present study. The values of stiffness and damping parameters for both the cases is given in the table 5.2.

Results with bump time included

Results of second case, in which the objective is minimization of the maximum vertical displacement for the whole time of travel, i.e, even the time when the wheels are on the bump are considered, are now presented. We again compare the results with those used by one of the automobile manufacturer (TELCO). Even in this case the results obtained are better as can be seen from figure 5.3. In table 5.3 the values of stiffness and damping parameters for the two cases is presented.

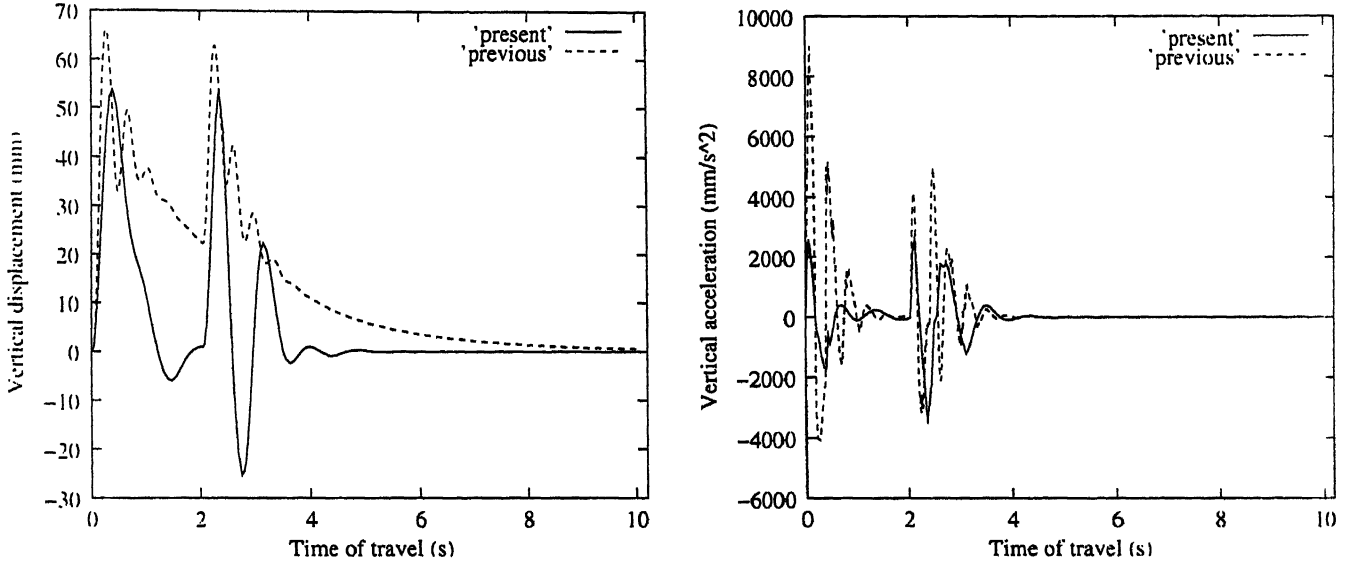


Figure 5.3: Comparison of present and previous results for the case in which whole of time of travel is considered.

Results	k_{fs}	c_f^a	k_{rs}^a	c_r^a	Transmissibility
Present	1.23	0.36	3.28	0.24	0.77
Previous (TELCO)	1.56	3.30	1.45	1.00	0.93

Table 5.3: Comparison of optimal values of stiffness and damping parameters for the case in which whole of time of travel is considered.

An interesting observation can be made when the results of the first and the second case are compared. It is observed that if the vehicle suspension is designed from the point of view of failure under stress, the second case is better but the first case leads to faster damping of vibrations. A comparison of the two results is presented now in figure 5.4

Looking at the values in the table 5.4 it can be seen that for the case in which bump time is excluded we have larger stiffness values as compared to those in the case when the bump time is also included while considering the objective function. So, in the former case we have higher displacement

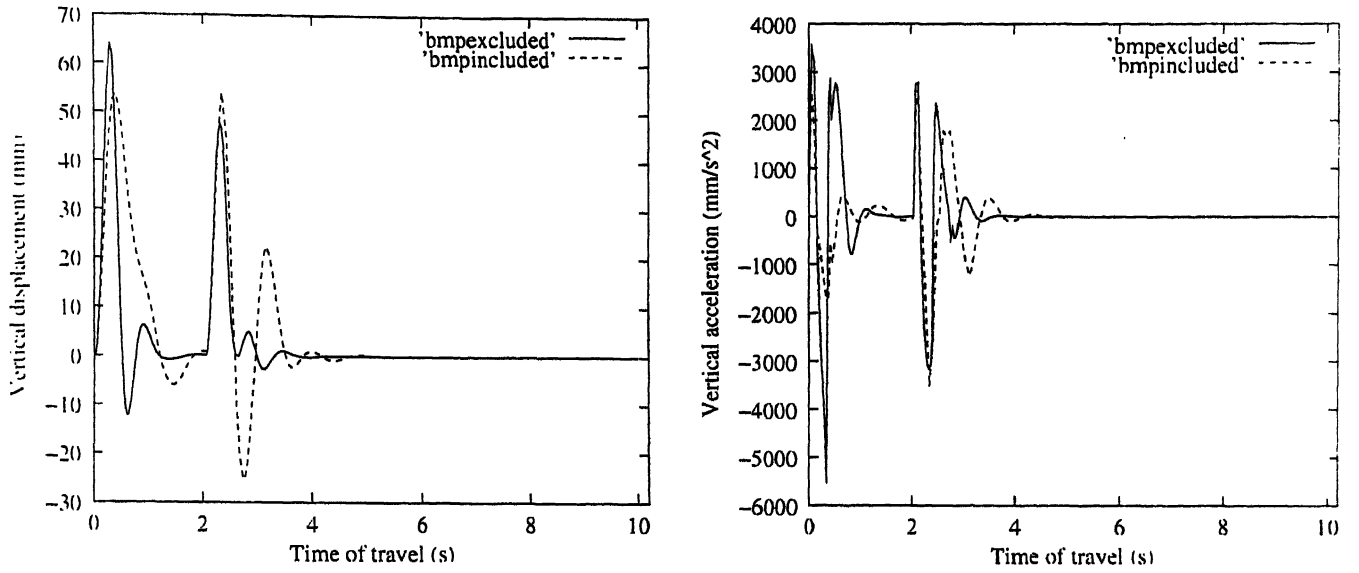


Figure 5.4: Comparison of two cases: one with bump time excluded and the other with bump time included.

or transmissibility values. Since, the damping is higher in the first case we have faster damping in the first case.

Results	k_{fs}	c_f^a	k_{rs}^a	c_r^a	Transmissibility
Bump time excluded	5.73	0.73	3.26	0.50	0.91
Bump time included	1.23	0.36	3.28	0.24	0.77

Table 5.4: Comparison of optimal values of stiffness and damping parameters for the two cases in which bump time is excluded or included.

5.1.2 Multi-objective optimization results

In the present study we have considered the minimization of transmissibility in bounce motion and minimization of vertical acceleration as the two objectives. The results were obtained in a single run of the NSGA-II algorithm used in conjunction with the adaptive step-size control Runge-Kutta algorithm. The various parameter values are as follows :

Population size : 300

Cross-over probability : 0.85

Mutation probability : 0.25

X-over distribution index : 20

Mutation distribution index : 100

Number of generations : 200

Results with car speed 5 km/h

In the multi-objective optimization we consider the case in which the bump time is also included, i.e. the whole time of travel is considered while evaluating the objective function. The reason for this is that in the transient vehicle response we are trying to minimize the maximum values of acceleration and displacement as they are the critical factors in the failure of parts under stress. The results of multi-objective optimization are presented now. We first show the set of optimal values in the objective function space in figure 5.5. These values are called the Pareto-front.

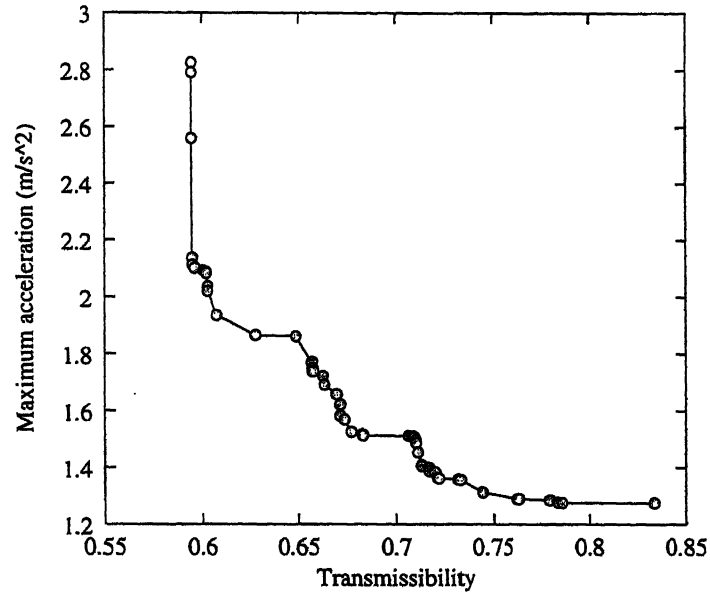


Figure 5.5: The Pareto front showing the optimal values in objective space for the car speed of 5km/h

Now, the designer can choose any set of values from this set depending on his specific requirements. The range of values can be better observed by looking at the two extreme values. The response based on these two extreme values is shown in the figure 5.6.

Results	k_{fs}	c_f^a	k_{rs}^a	c_r^a	Transmissibility	Max acceleration (m/s ²)
Minimum transmissibility	0.50	0.10	0.69	0.327	0.60	2.8
Maximum transmissibility	0.53	0.13	0.669	0.135	0.84	1.27

Table 5.5: Optimal values of stiffness and damping parameters with car speed 5 km/h

From table 5.5 we can see that the range of acceleration and transmissibility is not large in case of car speed of 5 km/h. The reason is that we have used a very low speed, i.e. 5 km/h and at such low

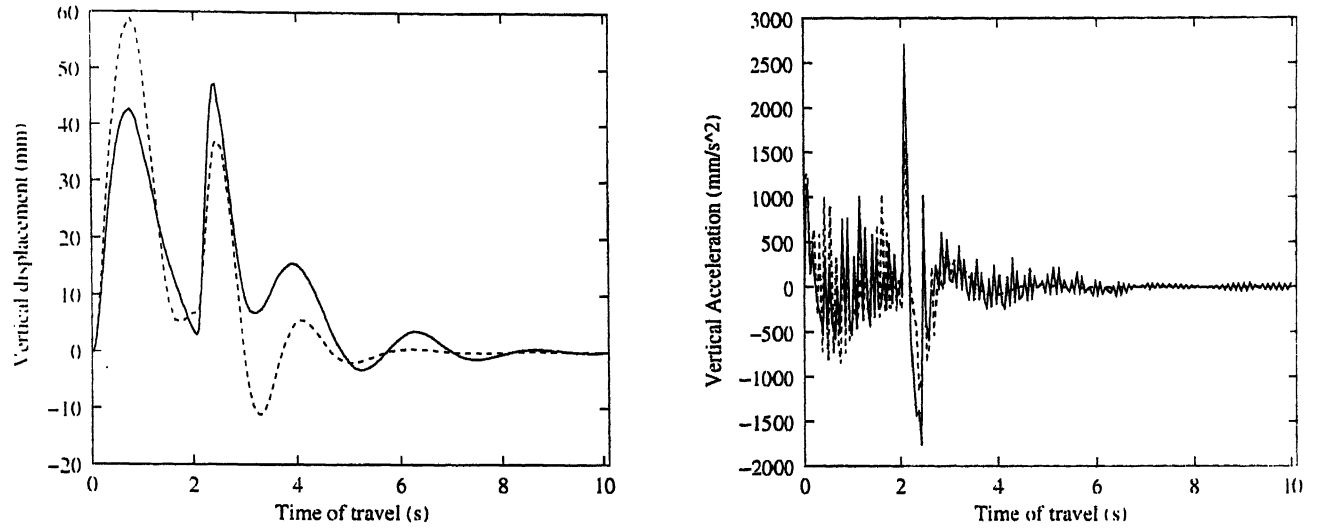


Figure 5.6: Comparison of two extreme values on the Pareto-front for the car speed of 5 km/h

speeds there are not many variations possible and mostly it is one solution instead of a set of solutions.

Results for single bump excitation at a car speed of 25 km/h

From figure 5.7, it can be seen that if we change the car speed to 25 km/h, other parameters remaining the same a wider range of solutions can be obtained as compared to those at car speed of 5 km/h. Figure 5.8, clearly shows the comparison of two extreme values of the Pareto-optimal front of the figure 5.7. In table 5.6, the respective values of stiffness and damping are given.

Results	k_{fs}	c_f^a	k_{rs}^a	c_r^a	Transmissibility	Max acceleration (m/s ²)
Minimum transmissibility	1.86	0.11	2.05	0.23	0.70	3.52
Maximum transmissibility	0.62	0.14	0.52	0.10	1.12	1.40

Table 5.6: Optimal values of stiffness and damping parameters with car speed 25 km/h

5.2 Results for three dimensional model

In the three dimensional model the objective function is subjected to three more constraints, i.e frequency constraints as was discussed in chapter 4. Also, when the vehicle speed is 50 km/h, we add another constraint for limiting maximum acceleration. The left and right suspension parameters are considered to be the same. The car parameters used in this model are the same as that used in the two dimensional model except $m_s = 1460$ kg, the left to right wheel distance is 1.462 m, and the rolling moment of inertia is $J_r = 1.864(10^9)$ kg.mm². Also, the width of the bump is taken as 2000 mm.

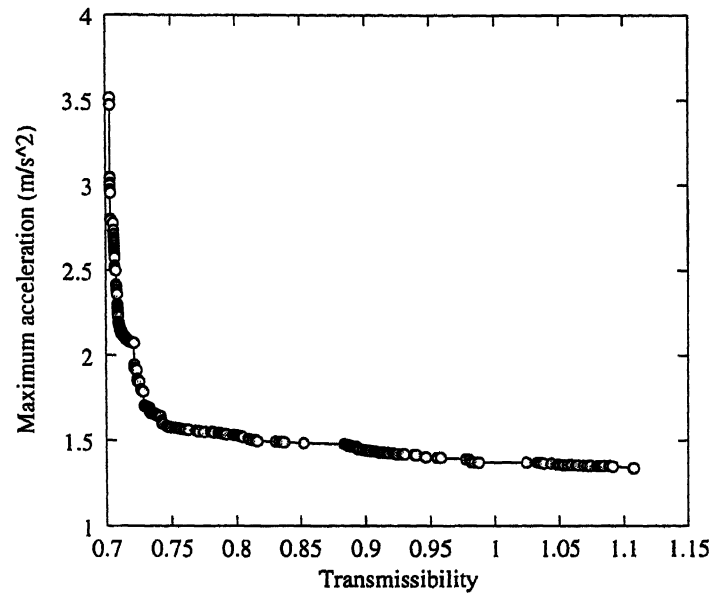


Figure 5.7: The Pareto front showing the optimal values in objective space with a car speed of 25 km/h

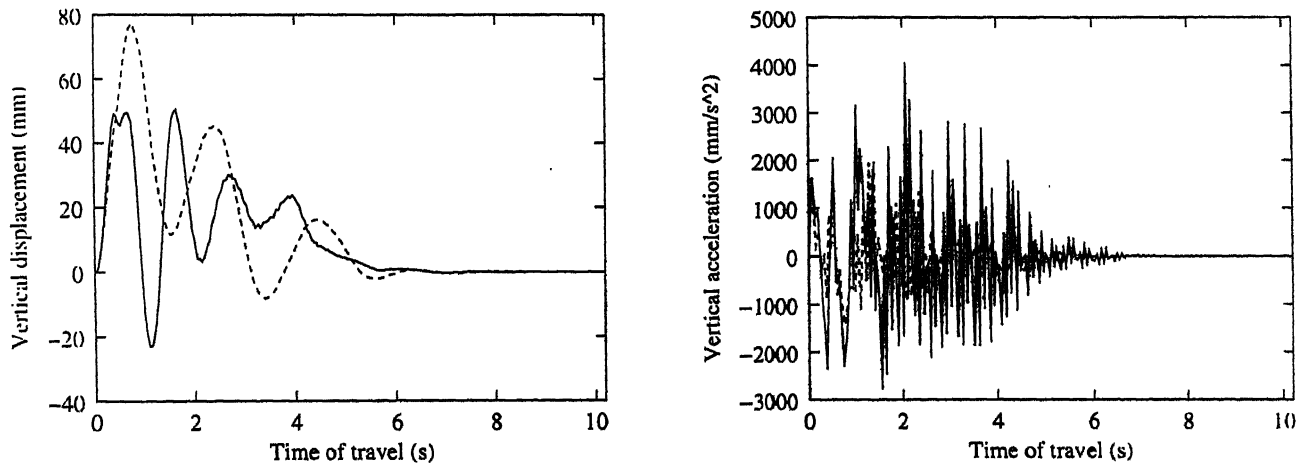


Figure 5.8: Comparison of two extreme values on the Pareto-front for the car speed of 25 km/h

5.2.1 Single objective optimization

In three dimensional model, different kinds of road excitations are considered. In the case of three dimensional model, we have also considered the pitching and the rolling motion when the car is excited by a rounded displacement step. Also, the profile of the bump has been changed from sinusoidal to profile represented by $1/2(1-\cos(2\pi x))$. Also, for all the cases two car speeds are considered, 5 km/h and 50 km/h.

Results for single bump excitation at a car speed of 5 km/h and 50 km/h

Firstly, the results for the case when the car experiences a single bump of the profile $1/2(1 - \cos(2\pi x))$ are presented in figure 5.9.

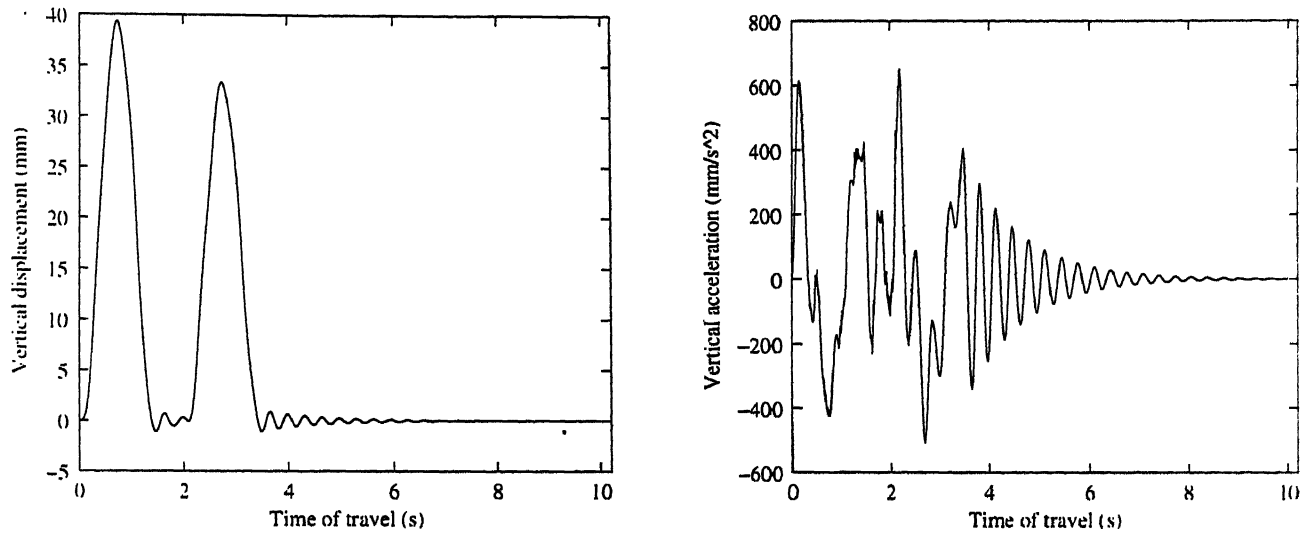


Figure 5.9: Results for single bump excitation at a speed 5 km/h

When the car passes over a bump of width 2 m, with a speed of 5 km/h it is observed that the sprung mass almost follows the bump, and the wheelbase filtering effect is not very predominant, as by the time the rear wheels come in contact with the bump, the vibrations due to the first wheel hitting the bump have almost died down. But, when the car speed is 50 km/h, the wheelbase filtering effect can be clearly seen. The vehicle response for single bump excitation in the case of car speed of 50 km/h, is shown in the figure 5.10.

Results	k_{fs}	c_f^a	k_{rs}^a	c_r^a	Transmissibility	Max acceleration (m/s ²)
Speed 5 km/h	1.17	2.76	1.24	5.21	0.56	0.62
Speed 50 km/h	1.49	1.05	0.86	0.26	1.48	9.00

Table 5.7: Optimal values of stiffness and damping parameters for single bump excitation

By studying table 5.7, we see that in the case of car speed the damping coefficient values are much smaller in comparison to those at car speed of 5 km/h. This can be understood because at higher speeds the higher the damping force the greater the disturbance fed into the sprung mass by any given road irregularity. For the speed of 5 km/h with the single bump the values of front, rear and pitch natural frequencies are 1.21 Hz, 1.35 Hz and 1.29 Hz respectively. Also, the maximum jerk value in

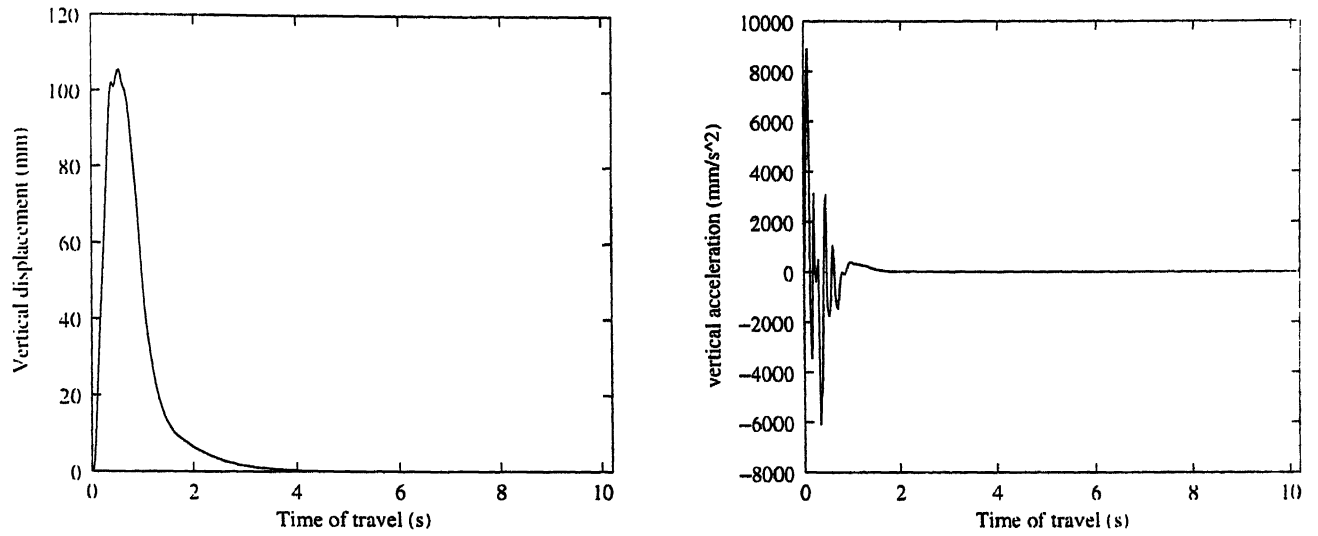


Figure 5.10: Results for single bump excitation at a speed 50 km/h

this case is about 6.4 m/s^3 . In the case of single bump excitation at car speed of 50 km/h the values of maximum vertical jerk, front frequency, rear frequency, and pitch frequency are 14.9 m/s^3 , 1.13 Hz, 1.37 Hz and 1.25 Hz respectively. So, in both the cases there is no constraint violation.

Results for three bumps excitation at car speeds of 5 km/h and 50 km/h

Next we consider three similar bumps in series, with the gap between the two bumps same as the bump width, i.e. 2000 mm. Again the optimization is performed for two speeds 5 km/h and 50 km/h.

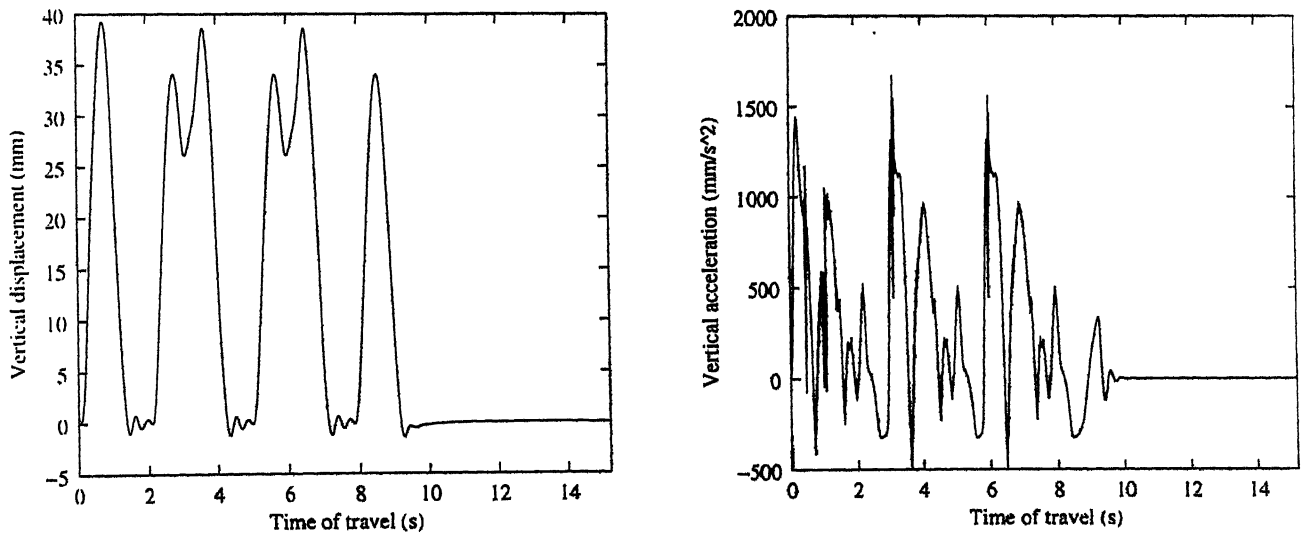


Figure 5.11: Results for three bumps excitation at a speed 5 km/h

Looking at the figures 5.11 and 5.12 for the three bump excitations at two speeds, we observe that for speed of 5 km/h there is little wheelbase filtering while in the case of speed 50 km/h there is significant wheelbase filtering. Also, at higher speed the displacement and acceleration values are higher as expected.

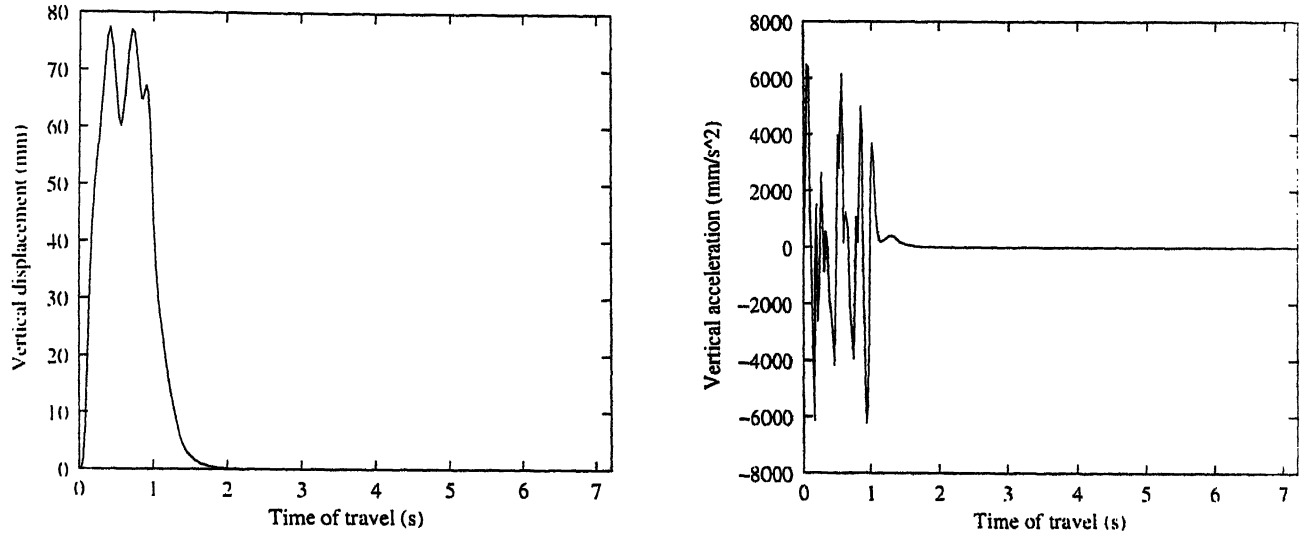


Figure 5.12: Results for three bumps excitation at a speed 50 km/h

Now looking at the values of stiffness and damping parameters in table 5.8, we see that at higher speed the stiffness values have increased and the damping values have reduced considerably. It is because the higher stiffness values are required to reduce the displacement and lower damping values do not feed much disturbance to the sprung mass. The values of front, rear and pitch natural frequencies in the case of car speed of 5 km/h are 0.84 Hz, 1.35 Hz and 1.14 Hz respectively. The values of front, rear and pitch natural frequencies for car speed of 50 km/h are 2.08 Hz, 2.38 Hz, 2.22 Hz respectively. Since, lower frequencies correspond to higher ride comfort it is obvious that the ride is more comfortable when the car speed is 5 km/h. However, to achieve such low frequencies, a softer suspension has been used, which asks for a compromise in ride handling, but then ride handling is not a problem at low speeds.

Results for rounded displacement step excitation at car speed of 5 km/h and 50 km/h with linear and non-linear damping

To study the effect of non-linear damping a more severe excitation function is required. So we have considered a rounded step function and a cubic damping term is added to the linear damping term in

Results	k_{fs}	c_f^a	k_{rs}^a	c_r^a	Transmissibility	Max acceleration (m/s ²)
Speed 5 km/h	0.56	2.75	1.24	0.86	0.54	1.60
Speed 50 km/h	4.5	0.87	2.92	0.68	1.10	6.50

Table 5.8: Optimal values of stiffness and damping parameters for three bumps excitation

the force expression. The coefficient of cubic damping term is taken to be negative and one-fourth of the linear damping term. We now present a comparison of the vehicle response with linear damping and cubic damping at two speeds 5 km/h and 50 km/h. A negative damping coefficient with numerical value one-fourth of that of linear damping coefficient has been employed.

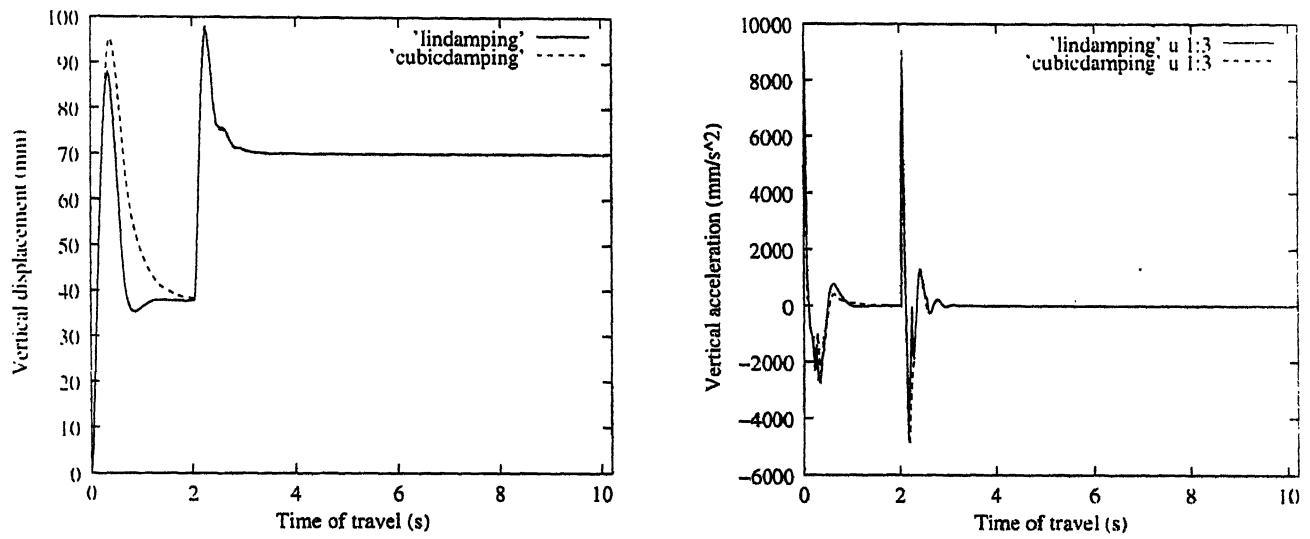


Figure 5.13: Results for rounded step excitation at a speed 5 km/h

It is evident from the figures 5.13 and 5.14 that the non-linear damping with the negative coefficient has worsened the vehicle's response. This non-linearity effect is more dominant at higher speeds. The values of stiffness and damping parameters for linear and cubic damping for the car speeds of 5 km/h and 50 km/h are presented in the tables 5.9 and 5.10 respectively.

5.2.2 Results of multi-objective optimization

Just like the two-dimensional case we consider the two conflicting objectives the transmissibility in the bounce motion and the vertical acceleration. Also, other conflicting objectives like pitching amplitude and pitching acceleration and rolling amplitude and rolling acceleration are considered. In all the cases

Results	k_{fs}	c_f^a	k_{rs}^a	c_r^a	Transmissibility
Linear damping	2.35	0.47	3.72	0.98	1.34
Cubic damping	1.41	0.59	3.82	0.95	1.40

Table 5.9: Optimal values of stiffness and damping parameters for rounded step excitation at speed 5 km/h

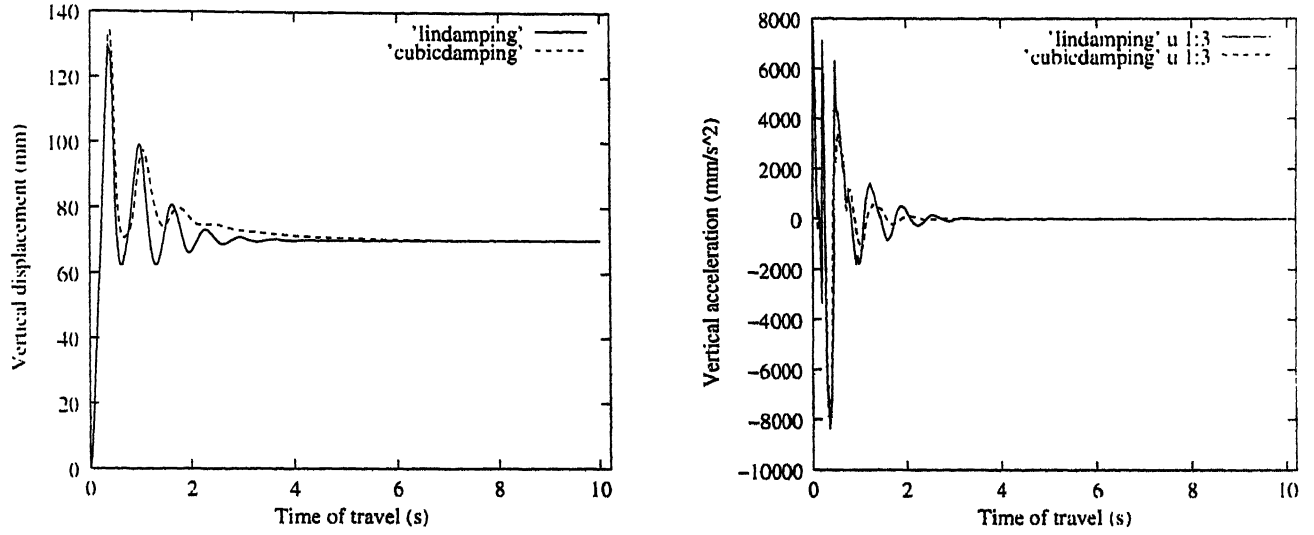


Figure 5.14: Results for rounded step excitation at a speed 50 km/h

Results	k_{fs}	c_f^a	k_{rs}^a	c_r^a	Transmissibility
Linear damping	4.77	0.25	3.02	1.50	1.74
Cubic damping	3.68	0.29	1.14	1.59	1.92

Table 5.10: Optimal values of stiffness and damping parameters for rounded step excitation at speed 50 km/h

the whole of the time of travel is considered. We observed that when the car speed is 5 km/h the range of transmissibility values is very small, in the case of single bump and a series of bump. This happens because the car speed is very small and we have increased the bump width to 2000 mm, so the car follows the bump smoothly and not many variations are available. So for this speed the RGA results are the best.

Results for single bump excitation at a car speed of 50 km/h

Now, we present the results of multi-objective optimization when the car is excited by a single bump which is of the same profile as was used in the single objective optimization. The speed of the car is 50 km/h. We start by presenting the Pareto-front obtained in this case in the figure 5.15. The two extreme solutions are plotted in the figure 5.17.

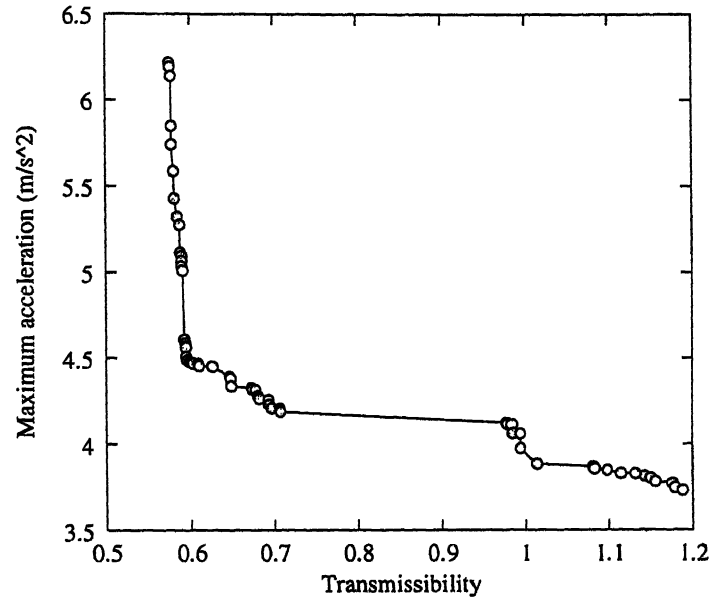


Figure 5.15: The Pareto front showing the optimal values in objective space for single bump at 50 km/h

Figure 5.16 clearly shows the exact position of the Pareto-optimal front in the feasible search space. The small dots in the figure represent the points which do not violate any of the constraints. The multi-objective optimization results presented in the table 5.11 point to a very interesting fact about the damping coefficients. It is seen that when acceleration is considered as one of the objectives the damping coefficients tend to move to the lowest minimum possible most of the times. The reason probably is that higher damping coefficients that the higher the damping force the greater the disturbance fed into the sprung mass by any given road irregularity, so the optimal solutions have damping values which are just enough to prevent undue persistence of vibrations.

The results presented in the table 5.11 clearly show that the higher stiffness values lead to lower displacements and higher accelerations and a softer suspension produces smaller accelerations. The value of front, rear and pitch frequencies corresponding to minimum transmissibility are 1.44 Hz, 2.50 Hz and 1.99 Hz respectively. So, in this case the maximum frequency constraint is active assuring us that the results obtained have a high probability of being the global optima. The front, rear and pitch frequency values for the maximum transmissibility case are 0.80 Hz, 1.57 Hz, 1.22 Hz respectively. Again, in this case the minimum frequency constraint is active and thus it can be said that the results are optimum. Also, the stiffer suspension corresponds to higher frequency values and the softer suspension corresponds

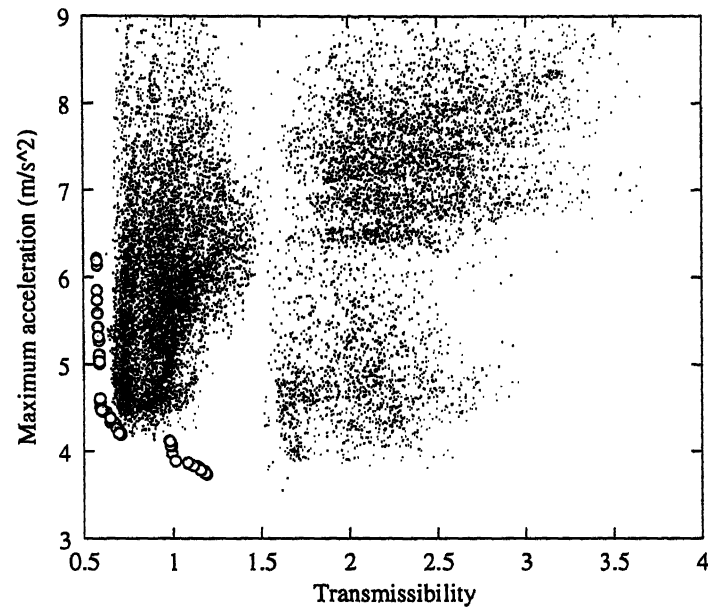


Figure 5.16: The position of the Pareto-optimal front in the feasible search space in case of single bump excitation at speed 50 km/h

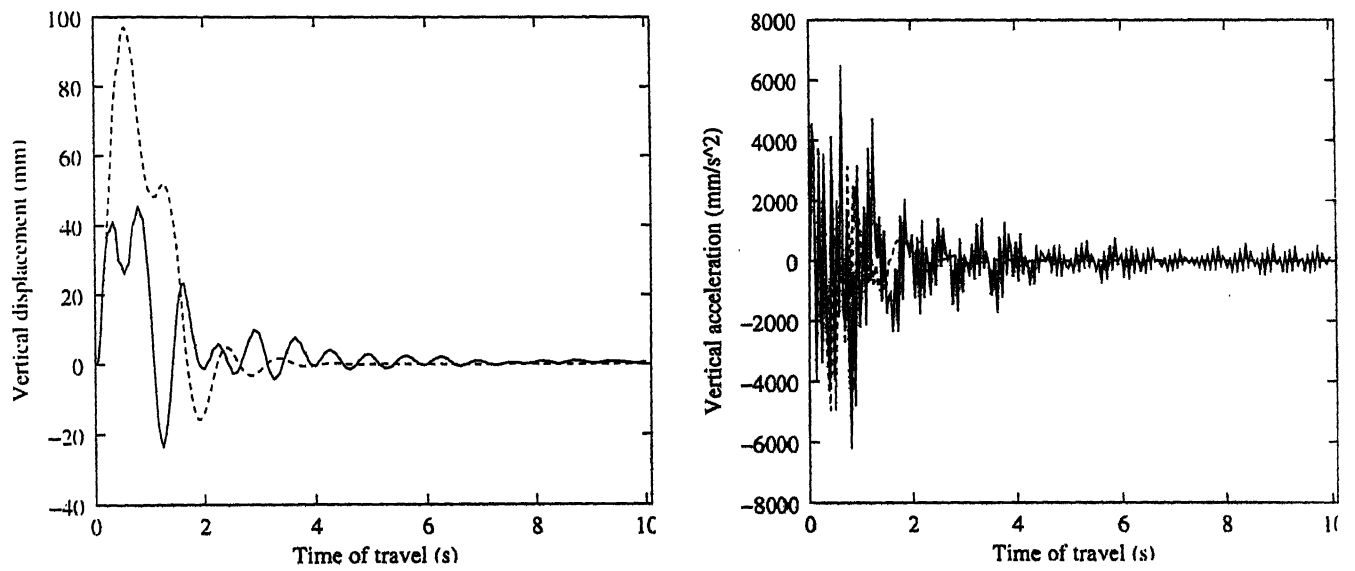


Figure 5.17: Results for single bump excitation at a speed 50 km/h

to lower frequency values.

Results	k_{fs}	c_f^a	k_{rs}^a	c_r^a	Transmissibility	Max acceleration (m/s ²)
Minimum transmissibility	4.95	0.13	1.40	0.10	0.58	6.3
Maximum transmissibility	1.97	0.17	0.44	0.16	1.19	3.75

Table 5.11: Optimal values of stiffness and damping parameters for single bump excitation at speed 50 km/h

Results for three bumps excitation at a car speed of 50 km/h

Next, we consider the excitation of car suspension with a series of three bumps equally spaced with the gap between them equal to the width of the bump. The car speed is taken to be 50 km/h.

The Pareto-front is shown in the figure 5.18. Also, the position of the Pareto-optimal front in the search space is shown in the figure 5.19.

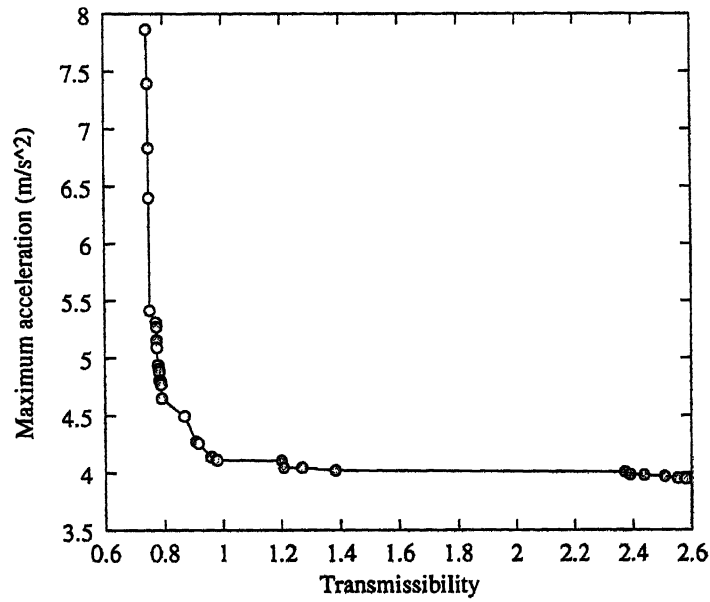


Figure 5.18: The Pareto front showing the optimal values in objective space for three bumps in series at 50 km/h

The two extreme responses obtained from the Pareto-optimal front are shown in the figure 5.20. In case of excitation of car suspension by a series of bump, the vibrations take a long time to die down, in the case of lower transmissibility and higher acceleration. The reason is that the vibrations produced by a single bump are further accentuated by other bumps in series. But, for higher transmissibility case, the effect of other bumps does not add to that of the first bump as the sprung mass has already been disturbed to a very displacement value. The two extreme solutions are given in the table 5.12. For the case of minimum transmissibility the front, rear and pitch frequency are 1.86 Hz, 2.50 Hz, 2.17

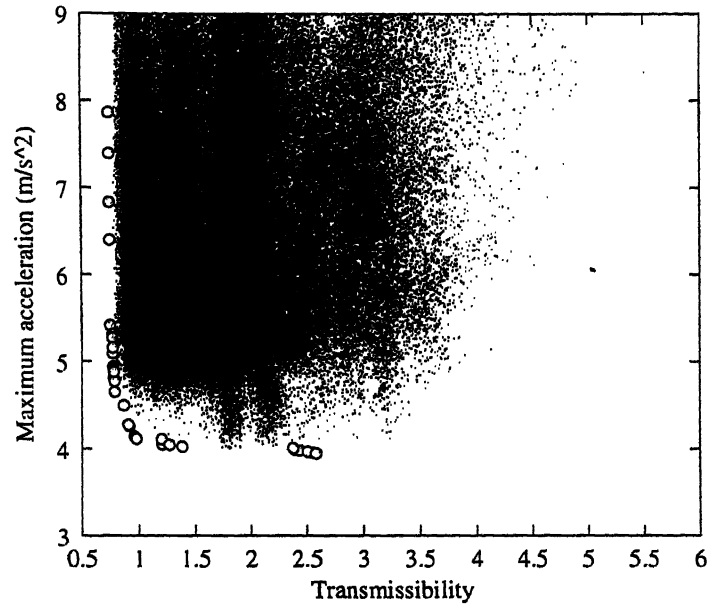


Figure 5.19: The position of the Pareto-optimal front in the feasible search space in case of three bumps excitation at car speed 50 km/h

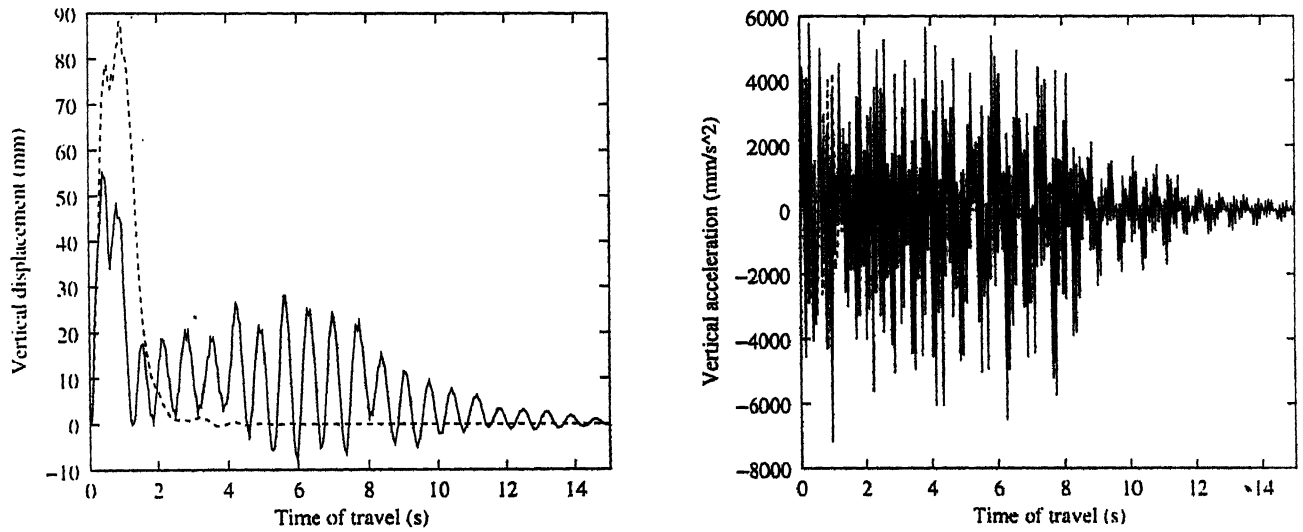


Figure 5.20: Results for three bumps excitation at a speed 50 km/h

Hz respectively. In the maximum transmissibility case the respective frequency values are 1.04 Hz, 1.90 Hz, and 1.50 Hz.

Results	k_{fs}	c_f^a	k_{rs}^a	c_r^a	Transmissibility	Max acceleration (m/s ²)
Minimum transmissibility	4.93	0.12	2.35	0.22	0.76	7.8
Maximum transmissibility	2.89	0.12	0.74	0.27	1.40	4.0

Table 5.12: Optimal values of stiffness and damping parameters for three bumps excitation at speed 50 km/h

Results for rounded displacement step excitation at 5 km/h 50 km/h

In the rounded displacement step excitation we consider both the car speeds 5 km/h and 50 km/h for bounce motion. The rounded displacement function as mentioned in chapter 4 has $\gamma = 50$, i.e. the excitation is more severe. Henceforth, in all the cases we have considered a cubic damping in addition to the linear damping term. The results for the bounce motion are now presented. For the car speed of 5 km/h the Pareto-optimal front is shown in figure 5.21. The comparison of extreme values is shown in the figure 5.22.

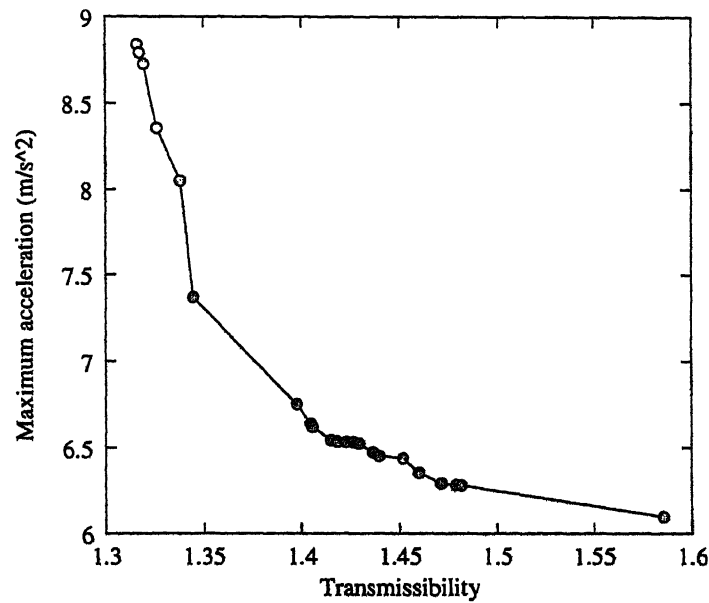


Figure 5.21: The Pareto front showing the optimal values in objective space for rounded displacement step at 5 km/h

From table 5.13 it can be noticed that the stiffness values are comparatively lower than those present in the previous cases. For minimum transmissibility value the front, rear and pitch frequencies are 1.91 Hz, 2.21 Hz, 2.05 Hz respectively. For maximum transmissibility case the respective frequency values

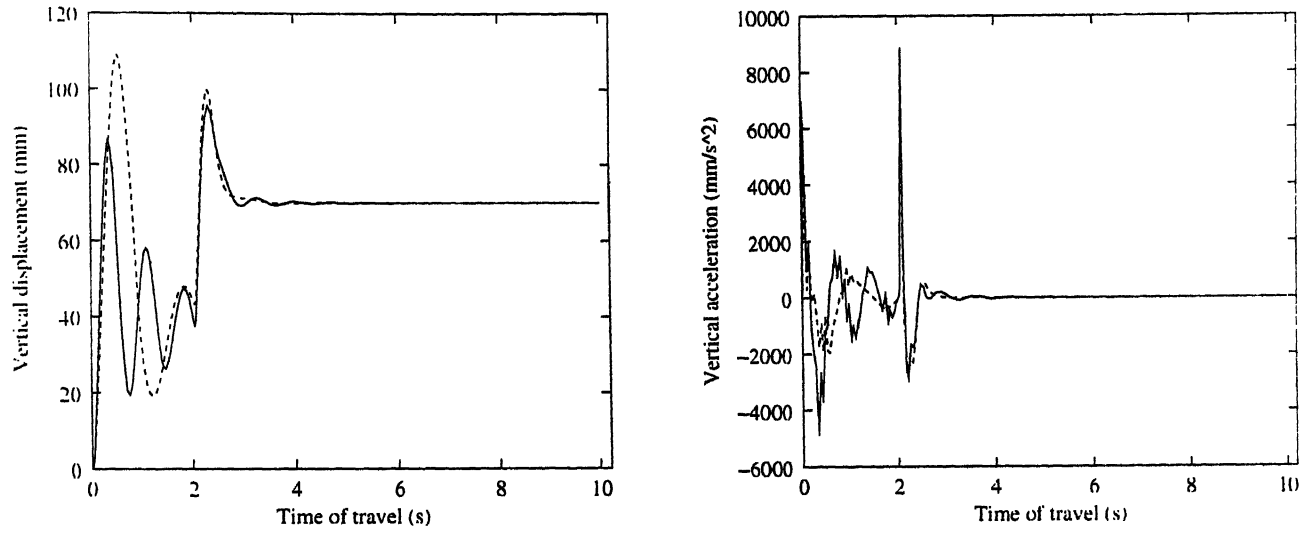


Figure 5.22: Results for rounded displacement step excitation at a speed 5 km/h

are 1.18 Hz, 1.77 Hz, and 1.53 Hz respectively.

Results	k_{fs}	c_f^a	k_{rs}^a	c_r^a	Transmissibility	Max acceleration (m/s ²)
Minimum transmissibility	3.88	0.19	2.46	0.64	1.31	8.83
Maximum transmissibility	1.11	0.18	2.11	0.54	1.58	6.09

Table 5.13: Optimal values of stiffness and damping parameters for rounded displacement step excitation at speed 5 km/h

In case of rounded step excitation at car speed of 50 km/h the Pareto-front has a wider range of transmissibility and acceleration values as shown in the figure 5.23. The extreme responses are shown in the figure 5.24. The extreme optimal solutions are given in the table 5.14. The front, rear and pitch frequency for minimum transmissibility case are 1.54 Hz, 2.49 Hz, 2.03 Hz respectively. The respective values for the case of maximum transmissibility are 0.87 Hz, 1.63 Hz, 1.27 Hz. It is observed that the damping coefficient values tend to be minimum and the various responses can be obtained by varying the values of the stiffness parameters with higher stiffness values corresponding to higher acceleration and lower displacement or transmissibility.

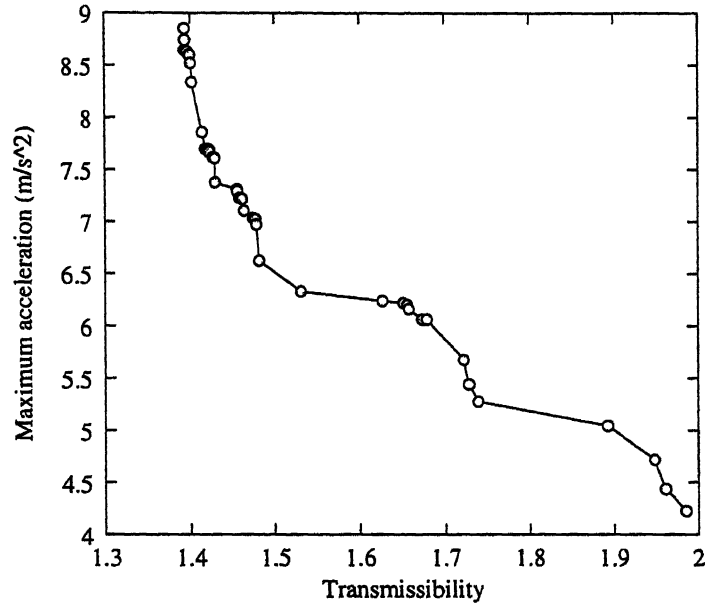


Figure 5.23: The Pareto front showing the optimal values in objective space for rounded displacement step at 50 km/h

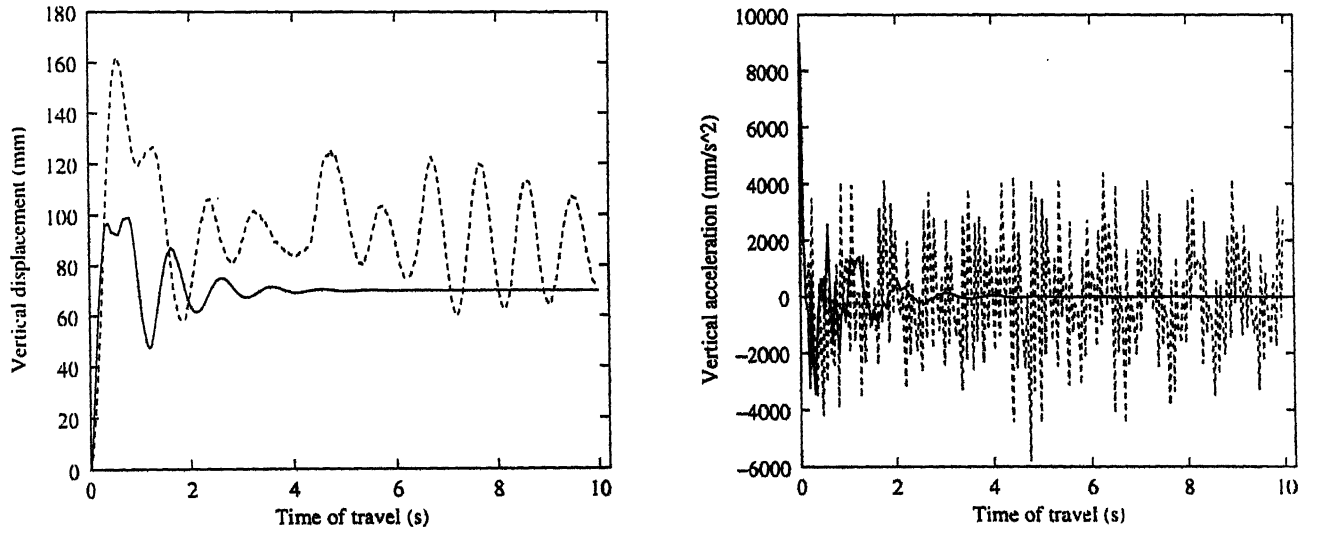


Figure 5.24: Results for rounded displacement step excitation at a speed 50 km/h

Results for pitching motion with rounded step displacement at a car speed of 50 km/h

Next, we consider another set of objectives i.e., pitching amplitude and pitching acceleration of the sprung mass. The excitation function is the rounded displacement step function and the car speed is

Results	k_{fs}	c_f^a	k_{rs}^a	c_r^a	Transmissibility	Max acceleration (m/s ²)
Minimum transmissibility	4.90	0.43	1.61	0.10	1.39	8.85
Maximum transmissibility	2.11	0.10	0.51	0.11	1.98	4.22

Table 5.14: Optimal values of stiffness and damping parameters for rounded displacement step excitation at speed 50 km/h

50 km/h. The obtained Pareto-front for the pitching motion is shown in the figure 5.25 and the two extreme responses are shown in the figure 5.26.

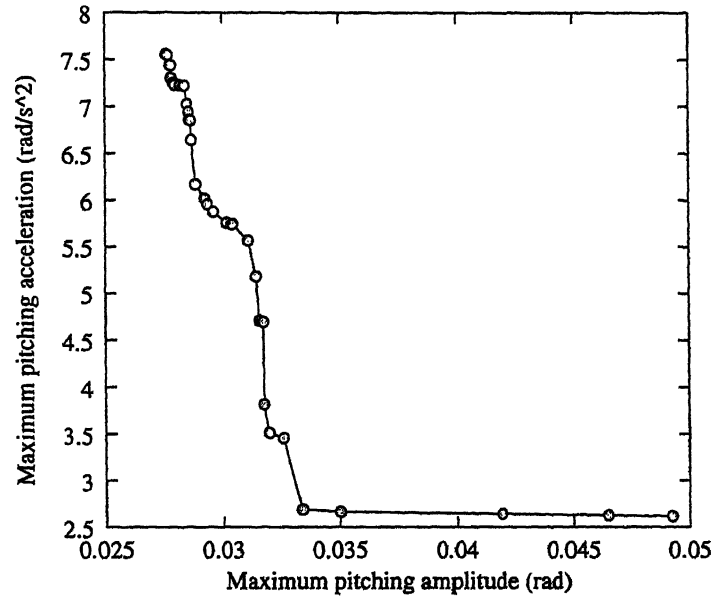


Figure 5.25: The Pareto front showing the optimal values in case of pitching motion for rounded displacement step at 50 km/h

From table 5.15 it can be made out that for pitching amplitude to be smaller the front suspension stiffness should be smaller than the rear suspension stiffness. This observation matches with the theory. Also, from the figures showing pitching motion, it is noted that for the faster dying down of pitching motion the rear damping co-efficient should have a high value. The front, rear and pitch frequencies for the minimum transmissibility case are 1.03 Hz, 1.17 Hz, 1.11 Hz respectively. The respective frequency values for the maximum transmissibility case are 0.87 Hz, 1.04 Hz, 0.95 Hz.

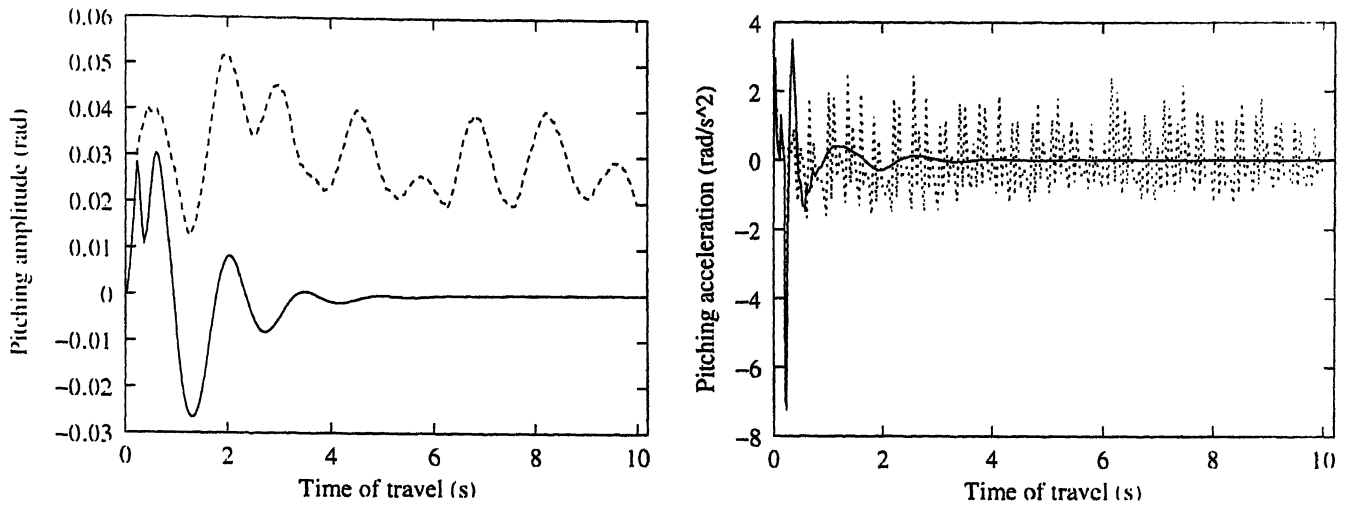


Figure 5.26: Results for rounded displacement step excitation in case of pitching motion at a car speed 50 km/h

Results	k_{fs}	c_f^a	k_{rs}^a	c_r^a	Pitching amplitude (rad)	Max acceleration (rad/s ²)
Minimum pitching amplitude	0.85	0.11	0.93	1.2	0.028	7.56
Maximum pitching amplitude	0.86	0.10	0.51	0.20	0.049	2.69

Table 5.15: Optimal values of stiffness and damping parameters for rounded displacement step excitation in case of pitching motion at speed 50 km/h

Results for rolling motion with a rounded step hole at a car speed of 50 km/h

In 3-D model we can consider the rolling motion of the sprung mass as well. So, optimization of the rolling motion is done for a special case. In this case we assume that, the right wheels of the car fall in a ditch which can be modelled as the negative of rounded displacement step function. The left wheels do not experience any kind of road excitation, and hence a rolling motion of the sprung mass takes place. The results of the optimization of rolling motion are presented now. The Pareto-optimal front for the rolling motion is shown in the figure 5.27. The extreme responses are shown in the figure 5.28.

From table 5.16 we observe that the stiffness values are hitting their lower bounds. The damping coefficient values are the deciding factor in minimizing the rolling motion. Higher damping coefficients lead to lesser rolling. All the three frequencies are very close to the lower bound, i.e., 0.8 Hz.

5.3 Conclusion

In the present study a further step is taken with respect to a systematical improvement of vehicle's dynamic behaviour. Before presenting the conclusion of the present work, it would be worthwhile to look

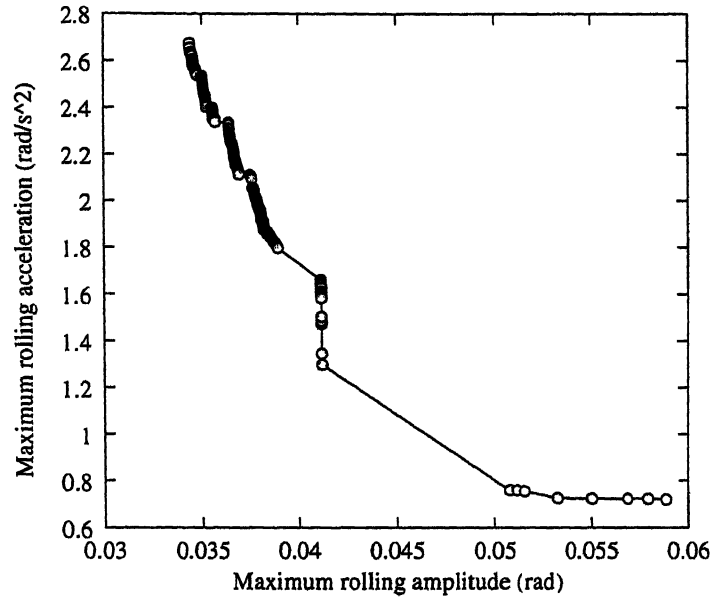


Figure 5.27: The Pareto front showing the optimal values in case of rolling motion for rounded displacement step at 50 km/h

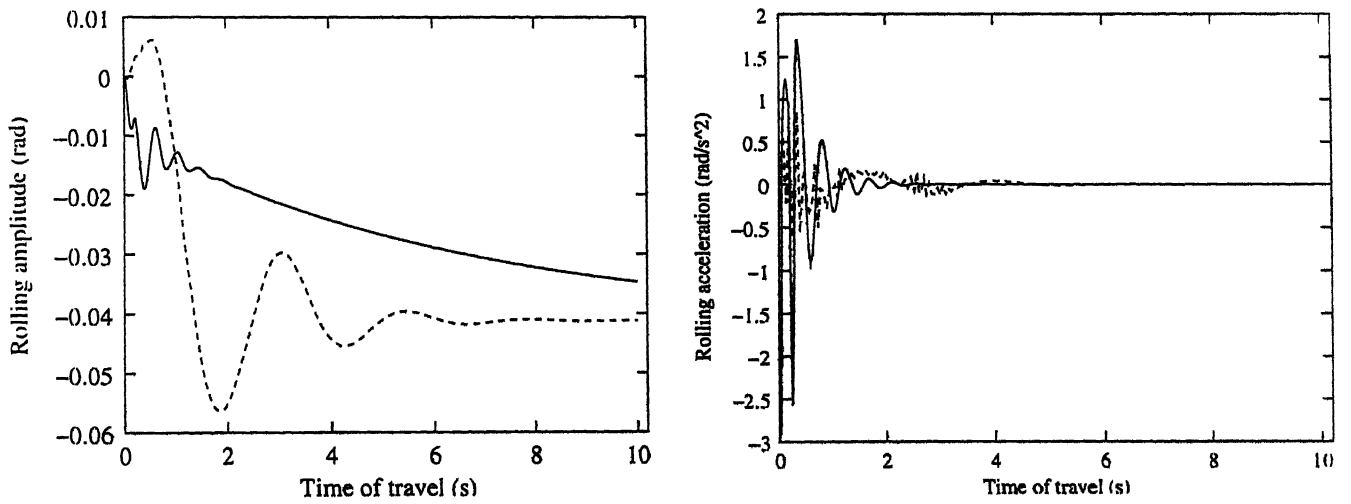


Figure 5.28: Results for rounded displacement step excitation in case of rolling motion at a car speed 50 km/h

at the present status of the optimization methods in the industry. This will help us better understand the aim of the present study. Three very important points refer to the general opinion of designers about the optimization procedures.

- Optimization algorithms are mathematical tools that cannot take into consideration the physical

Results	k_{fs}	c_f^a	k_{rs}^a	c_r^a	Rolling amplitude (rad)	Max acceleration (rad/s ²)
Minimum rolling amplitude	0.51	4.55	0.53	1.93	0.034	2.67
Maximum rolling amplitude	0.51	0.12	0.52	0.11	0.059	0.72

Table 5.16: Optimal values of stiffness and damping parameters for rounded displacement step excitation in case of rolling motion at speed 50 km/h

or engineering aspects of the problem and so, they give us mathematical solutions, that are mathematically correct. but most of the time are of no practical interest to the engineer.

- Physical or engineering aspects of the problem must be taken into consideration by incorporating appropriate constraints in the formulation of the optimization problem.
- Optimization algorithms may be fouled very easily by considering a local minimum. To reach the global optimum a number of runs have to be made from different initial points. This leads to high computation cost and time.

With these points in mind, we proceeded to optimize the ride behaviour of the vehicle. From the present study following conclusions can be made.

- GAs can be easily coupled with numerical integration technique to solve the problems of dynamic engineering design. In the present study, the combination of RGA and NSGA-II with adaptive step-size control Runge-Kutta method has worked desirably.
- One of the major problems in optimizing the ride behaviour of a vehicle has been the lack of optimization tools which are less time consuming, since the evaluation process involves iterative numerical integration of differential equations of motion. This problem has been effectively overcome by the use of genetic algorithms.
- Most of the conventional techniques are unable to handle the problem in which the search space is highly constrained, since the penalty function methods used distort the objective function. A good way of constraint handling in the RGA and NSGA-II algorithms has made the use of a number of constraints in the present study possible.

- This study focusses mainly on the application of multi-objective genetic algorithm, i.e. NSGA-II, to the dynamic system design. Since, in most of the practical design problems, dynamic systems have to be optimized with respect to several conflicting specifications and several conflicting specifications and several different design are acceptable as optimal with respect to the same set of specification, the present work brings forth an effective optimization strategy for the design engineer. This strategy can be easily applied to many multi-body dynamics problems.

Also, a few features of the car suspension design which came forward or were reaffirmed are as follows :

- Two conflicting objectives of ride are the minimization of vehicle's displacement and acceleration respectively. The designer has to strike a balance between these two objectives. A set of optimal values provide the designer with a choice and he can select a particular solution which meets his needs.
- It is observed that the softer springs lead to lower natural frequencies and lower accelerations but the displacement values higher as compared to those of the stiffer springs. It is desirable to have as soft a suspension as possible, but the stiffness values have to be restricted to a lower bound because of rattle space constraints and to improve the handling characteristics of the vehicle.
- It is observed that the higher stiffness values are restricted by the upper limit of maximum allowed frequency. In case of most cars the natural frequency is kept below 2 Hz. Performance cars on which ride is sacrificed for the handling benefits of a car suspension, have natural frequency upto 2.5 Hz.
- The amount of damping required is a compromise between that needed due to prevent undue persistence of a vibration at natural frequency excited by a single disturbance, which also prevents the build up of excessive amplitude of a forced vibration due to a series of impulses, and the uncomfortable fact that the higher the damping force the greater the disturbance fed into the sprung mass by any given road irregularity. We usually obtained low values of damping coefficients. However, too low damping cannot be used as it is insufficient to control wheel hop oscillations which compromise road holding behaviour.

- Also, another important feature i.e., non-linear damping has been used in the present study. It was found that non-linearity of dampers comes into play only in the case of severe shock loading. So, we have used a rounded displacement step to study the effect of cubic damping and then optimization has been performed on suspension with non-linear dampers. It is observed that the negative non-linear damping coefficient worsens the displacement response.

As a final note one might hypothesize that the ride engineer's goal should generally be to eliminate all vibrations in a vehicle. Even though this will never be possible in a motor vehicle, it does give direction to the development effort. Yet there are two contrary phenomena that must be dealt with. First, the elimination of one vibration will always expose another lesser annoyance. Second, in the limit, elimination of all vibrations is not desirable as vibrations are the source of road feel considered to be essential feedback to the driver of a motor vehicle.

5.4 Scope for the future work

The present work is one step towards the effective use of multi-objective genetic algorithms to the dynamics design problems. It provides a new strategy in which optimization algorithms effectively couple with numerical integration technique to optimize the ride dynamics of vehicle. However, as suggested the vehicle dynamics is a very complex issue and it can be viewed from different perspectives. Also, other fields of engineering design should get encouraged to use multi-objective genetic algorithms as an optimization tool. A few suggestions are put forth for the future work related to this topic.

- Other conflicting parameters like ride handling and ride comfort can be considered. Also, we can consider the conflict between pitch and the bounce motion of the vehicle for multi-objective optimization.
- GAs can be used in conjunction with finite element models. This way a problem which combines sizing (stiffness and damping properties of elements) and geometry (nodal co-ordinates) optimization can be tackled.
- Another field of interest is the inclusion of kinematic control in vehicle handling and the influence of the tyre characteristics on the vehicle's behaviour.

5.5 Closure

In this chapter the results of optimization of a car suspension system are produced. Two dimensional model and three dimensional models have been dealt separately. First the results of single objective optimization using real-coded GA are presented and then the optimization results of multi-objective optimization results using NSGA-II are presented. Then the conclusion of the whole study is given in brief. The chapter ends with some suggestions for future work related to this topic.

Bibliography

- [1] Deb, K., Saxena, V.,(1994). *Car suspension design for comfort using genetic algorithms*. Kanpur: Indian Institute of technology Kanpur, India.
- [2] Deb, K., Agrawal, R.B.(1995). Simulated binary cross-over for continuous search space. *Complex Systems*, 9, pp. 115-148.
- [3] William, H.P., Teukolsky, S.A., Vetterling, W.T., Flannery, B.P.,(1996) *Numerical recipes in C. second edition* Cambridge university press.
- [4] Deb, K., Pratap, A., Agrawal, S. and Meyarivan, T. (2000). A fast and elitist multi-objective genetic algorithm: NSGA-II. Technical Report No. 2000001. Kanpur: Indian Institute of Technology Kanpur, India.
- [5] Deb, K., Agrawal, S., Pratap, A., Meyarivan, T. (2000). A Fast Elitist Non-dominated sorting genetic algorithm for multi-objective optimization: NSGA-II. *Proceedings of the Parallel Problem Solving from Nature VI Conference*, pp. 849–858.
- [6] Chandra Shekhar, N., Hatwal H., Mallik, A.K., (1999). Performance of non-linear isolators and absorbers to shock excitations. *Journal of sound and vibration* 227(2), pp. 293-307. Kanpur: Indian Institute of Technology Kanpur, India.
- [7] Spentzas, C.N.(1993). *Optimization of vehicle ride characteristics by means of Box's method*. United Kingdom.
- [8] Demic, M.,(1989). Optimisation of the elasto-damping elements of a passenger car by means of a modified Nelder-Mead method. *International Journal of Vehicle Design*, vol. 10, no. 2, United Kingdom.
- [9] Wimmer., J., Rauth, J.(1996). Multicriteria optimization as a tool in the vehicle's design process. *IUTAM symposium on optimization of mechanical systems* pp. 333-340.

- [10] Markine. V.L., Meijers, P., Meijaard, J.P., Torpov, V.V., (1996). Optimization of the dynamic response of linear mechanical systems using a multi-point approximation technique. *IUTAM Symposium on optimization of mechanical systems*pp. 189-196
- [11] Bestle. D., Eberhard, P.,(1999), *Dynamic System Design via Multicriteria Optimization*. Germany : Institute B of Mechanics, University of Stuttgart.
- [12] Guest, J.J..1925,*Book : The main free vibration of an autocar*London.
- [13] Gillespie. T.D.. *Book : Fundamentals of Vehicle Dynamics*
- [14] Steed. N.. *Book : The motor vehicle, Chapter 33*
- [15] Chandra Shekhar, N., Hatwal H., Mallik, A.K.,(1998). Response of non-linear dissipative shock isolators. *Journal of sound and vibration* 214(4),pp. 589-603. Kanpur: Indian Institute of Technology Kanpur,India.
- [16] Fonseca. C. M. and Fleming, P. J. (1993). Genetic algorithms for multi-objective optimization: Formulation, discussion, and generalization. *Proceedings of the Fifth International Conference on Genetic Algorithms*. 416-423.
- [17] Deb, K. (1999) Multi-objective genetic algorithms: Problem difficulties and construction of test Functions. *Evolutionary Computation*, 7(3), 205-230.
- [18] Horn, J. and Nafploitis, N., and Goldberg, D. E. (1994). A nichedPareto genetic algorithm for multi-objective optimization. *Proceedings of the First IEEE Conference on Evolutionary Computation*. 82-87.
- [19] Deb, K.,(2000). An efficient constraint handling method for genetic algorithms.*Computer Methods in Applied Mechanics and Engineering* 186, pp. 311-338
- [20] Deb., K. (2000) An efficient constraint handling method for genetic algorithms. *Computer Methods in applied mechanics and engineering*, 186, 311-338.
- [21] Srinivas, N. and Deb, K. (1995). Multi-Objective function optimization using non-dominated sorting genetic algorithms. *Evolutionary Computation*(2), 221-248.
- [22] Crolla, D.A.,(1996) Vehicle dynamics—Theory into practice. *IME journal, Automobile division chairman's address*
- [23] Zitzler, E. (1999). Evolutionary algorithms for multi-objective optimization: Methods and applications. *Doctoral thesis ETH NO. 13398*, Zurich: Swiss Federal Institute of Technology (ETH), Aachen, Germany: Shaker Verlag.

- [24] Zitzler, E., Deb, K., and Thiele, L. (2000). Comparison of multi-objective evolutionary algorithms: Empirical results. *Evolutionary Computation Journal*, 8(2), 173-196.
- [25] Zitzler, E. and Thiele, L. (1998). An evolutionary algorithm for multi-objective optimization: The strength Pareto approach. *Technical Report No. 43 (May 1998)*. Zürich: Computer Engineering and Networks Laboratory, Switzerland.

A133717

**The book is to be returned on
the date last stamped.**

This image shows a blank sheet of primary-ruled paper. It features a series of horizontal dotted lines spaced evenly down the page. A single vertical solid line runs from the top to the bottom of the page, acting as a central margin or midline. The paper is otherwise white and contains no other markings or text.

A133717

11-55717

TH

ME/2001/11

A14-0